Elemental and structural analysis with SEM-EDX of hydrochars obtained from hydrothermal carbonisation of different organic materials.

Diplomarbeit

von

Andreas Clementi

Matrikelnummer: 0940760

zur Erlangung des Akademischen Grades Diplomingenieur (Dipl.-Ing.)

Masterstudium Biotechnologie

Kennzahl: 066418

Christoph Pfeifer, Univ.Prof. Dipl.-Ing. Dr.techn

Gregor Tondl, Dipl.-Ing. Dr.

eingereicht am: 14.12.2015

Institute of Chemical and Energy Engineering

Department of Material Sciences and Process Engineering

Eidesstattliche Erklärung

Ich erkläre hiermit ehrenwörtlich, dass ich die vorliegende Arbeit selbstständig verfasst, andere als die angegebenen Quellen nicht verwendet, und die wörtlich oder inhaltlich entnommenen Stellen aus den benutzten Quellen als solche kenntlich gemacht habe.

Unterschrift:

Wien, am 14.12.2015

Acknowledgement:

Firstly, I would like to express my gratitude to my advisor Gregor Tondl for the continuous support of my study, for his patience and motivation. Then I would like to thank my supervisor Prof. Pfeifer, for granting my request for this study and most importantly for stirring up my curiosity for hydrothermal processes. Furthermore, I have to thank Prof. Pum for supporting my idea to use the SEM-EDX, which was one of the things I wanted to achieve since 2012, where I was working for the first time with a TEM. In addition I would like to thank Patrizia Stutzenstein, for granting me access to the HTC reactor, guiding me the first months of my thesis and leading my attention to the ELLS scientific student conference 2015.

Lastly my gratitude goes to all my co-workers, lab mates, friends and family members who supported me during this period.

Kurzfassung:

Hydrothermale Karbonisierung von Biomasse zu Hydrokohle hat das Potential ein umweltfreundlicher Prozess mit vielen Anwendungsmöglichkeiten zu werden. Neben der Verwendung als Energieträger, gibt es Ansätze Hydrokohle in umwelt-technischen-, katalytischen-, elektrotechnischen- und landwirtschaftlichen Bereichen zu verwenden. Da hydrothermale Karbonisierung von Biomasse ein äußerst komplexer Prozess ist, der noch nicht gänzlich charakterisiert ist, wird in dieser Studie versucht, einen Einblick in Reaktionsmechanismen und Vorgängen an und in Partikeln zu geben. Dafür wurden kohlenstoffhaltige Materialen mit einem 1,5 Liter Reaktor bei 180°C und autogenem Druck erzeugt. Als Ausgangsmaterial wurden Pistazien Schalen, Bambus Stäbchen, Tannennadeln und Gärreste aus Biogasanlagen verwendet. Um einen detaillierten Einblick in die chemische und strukturelle Zusammensetzung der Kohlen zu erlangen, wurden die Materialien mit einem SEM-EDX analysiert. Strukturell konnten kohlenstoffhaltige Sphären an der Oberfläche der Kohlen identifiziert werden, die einzigartig für die hydrothermale Karbonisierung sind. Diese µm große Sphären entstehen durch Dehydration, Kondensation und Polymerisation, ihre Form und Größe hängen dabei stark vom Ausgangsmaterial ab. Mit der energiedispersiven Röntgen Spektroskopie wurden Querschnitte von Partikeln mit unterschiedlichen Verweilzeiten auf O/C Verhältnisse analysiert. Als Modell wurde das Thiele Modul herangezogen, welches das Verhältnis von Reaktivität zu Diffusivität beschreibt. Es zeigt sich, dass das Modell zu den gemessenen O/C Profilen von Pistazienschalen und Bambusstäbchen passt und welches die Bestimmung der Thiele Module ermöglicht. Die gemessen Thiele Module liegen in einem Bereich von 1.61 ± 0.027 bis 1.19 ± 0.019. Dies soll beweisen, dass durch Diffusionsphänomene Reaktionsgeschwindigkeit der hydrothermalen Karbonisierung verringert wird. In Zukunft soll diese Methode durch den Einsatz von verschiedenen Partikelgrößen weiter abgesichert werden.

Abstract:

The carbonisation of biomass to hydrochar has the potential to become an environmentally sound conversion process for the production of a wide variety of products. Besides the use for the production of hydrochars as energy carriers, there are discussions about using hydrochars for environmental, catalytic, electronic and agricultural applications. Since hydrothermal carbonisation of biomass is highly complex and not yet fully understood, this study aims to elucidate the reactions occurring during the process at specific process parameters. Therefore carbonaceous materials were synthesised with a 1.5 litre reactor at 180°C and autogenic pressure using different feed materials such as pistachio shells, bamboo sticks, fir needles and biogas slurry. To gain a detailed insight into the chemical and structural properties, carbonaceous hydrochar materials were characterized by SEM imaging and EDX analysis. Structurally, carbon-rich spheres were detected on the surface of the hydrochars; size and shape of those carbon spheres strongly depend on the properties of the feed materials. The formation of these µm-sized spheres through hydrothermal carbonisation of biomass is the consequence of dehydration, condensation, or polymerization and aromatization reactions. Chemically, the atomic O/C profiles of cross sections obtained from different hydrochars were determined. Then, the Thiele module is used as a model for the observed O/C profiles, which describes the relation of reactivity to diffusivity of a reactant into a pore. It is shown, that this model fits to the EDX data and therefore it was used to calculate the Thiele Modules, which range from 1.61 ± 0.027 to 1.19 ± 0.019. This should proof, that hydrothermal reactions are hindered by diffusion and thereby reducing its reaction rate. In order to further verify this method, an analysis of different particle sizes is proposed.

Content:

1. Introduction

In the beginning of the twentieth century, many industrialised materials such as solvents, fuels, fibres and chemical products were made from plant and crop based resources. Unfortunately, this is no longer the case, because nowadays most of the industrial materials such as fuel, polymers, chemicals, fertilisers, carbons, pharmaceuticals, packing, construction, and many others, are being manufactured from fossil-based resources. This revolution started slowly in 1847 when James Young invented the distillation of kerosene from petroleum.

Until today, the demand for crude oil and other fossil-based resources is rising, but at the same time the resources are rapidly diminishing. Besides the scarcity of fossil-based resources, which often are reasons for conflicts, the use of such products usually end up as CO_2 in the Earth's atmosphere. Several important findings from climate research have been confirmed in the recent years and have finally been accepted as facts by the scientific community, which include the rapid increase in the CO_2 concentrations in the atmosphere during the last 150 years from 228 ppm to the 2007 level of 383 ppm, rising sea levels of 3 cm per decade and acidification of oceans (Rahmstorf et al. 2010). These facts show consequences of anthropogenic activities – consequences which still can be reversed. Therefore Intergovernmental Panel on Climate Change (IPCC) suggests the strategy of climate change mitigation by reducing anthropogenic emissions of greenhouse gases which include switching to low-carbon energy sources such as renewable and nuclear energy, expanding forests and other CO_2 sinks, increasing energy efficiency of industrial processes, insulation of buildings and other activities (IPCC 2011). Another important task is the shift from petroleum hydrocarbons to bio-based feedstock, which provides remarkable opportunities for the chemical processing industry and enables production of sustainable materials with defined properties (Green et al. 2012). Since biomass is the most abundant renewable resource on Earth, it would be beneficial to develop new starting materials from biomass from an industrial point of view (Koopmans 2006).

One important approach is the production of carbon materials, which are synthesised from renewable and highly abundant precursors. At the same time consuming as little energy as possible and avoiding the use and generation of toxic and polluting substances. Furthermore, they should perform an important technological or ecological task. In the last years, a large number of new carbon materials with well-defined nanostructures have been synthesised by

various physical and chemical process, such as fullerenes, carbon nanotubes (CNTs), graphitic onions, carbon coils, carbon fibres, and others (Titirici 2013). Three of those have been recognised with major awards: fullerenes (1996 Nobel Prize in Chemistry), CNTs (2008 Kvali Prize in Nanosciences), and graphene (2010 Nobel Prize in Physics). Unfortunately these carbon materials have been synthesised from fossil based precursors and energy-consuming methodologies which are producing toxic by-products. In order to protect our environment and to avoid the causes of global warming mentioned above, novel and sophisticated processes are needed to produces such carbon materials. One possible way to carbonise biomass under mild conditions would be hydrothermal carbonisation (HTC) where biomass is treated with subcritical water at temperatures around 180-250°C and autogenous pressure. One of the most significant advantages of the HTC is that the biomass does not need to be dried; it has been reported, that biomass with water content up to 96% has been effectively carbonised (Schneider et al. 2011).

1.1 History of HTC

Hydrothermal carbonisation is not a new field of research but has its origin in the first decades of the twentieth century when it was used to understand the mechanisms of natural coalification. Friedrich Bergius (1884-1949) was doing research on topics that are currently of extreme importance for finding alternative fuels to the fossil-based fuels. However his experiments failed to reach desired reaction velocities, which would have made such a conversion of commercial interest. At that time, his research about transforming coal into a liquid fuel was much more popular, most probably due to the upcoming Second World War and the efforts to be self-sufficient on oil.

Figure 1. Friedrich Karl Rudolf Bergius (11 October 1884 – 30 March 1949)

Nevertheless Friedrich Bergius was the first to produce so called hydrochars and to discover, that at temperatures above 200°C the biomass precursors had to be in close contact with water in order to prevent decomposition into gases (Titirici 2013). For his contributions to many studies regarding reactions under high pressure, Bergius and Carl Bosch was awarded with the Nobel Prize of Chemistry in 1931.

In the end of the twentieth century HTC regained scientific interest with topics such as hydrothermal degradation of organic matter (Bobleter 1994), synthesis of basic chemicals as well as liquid and gaseous fuels (Overend et al., 1985). In recent years, research activities where focused on the production of solid carbonaceous materials, termed hydrochar. The German researchers Maria-Magdalena Titirici and Markus Antonietti performed state-of-the-art experiments which helped to understand the process much more in detail. Recent discoveries where, that the process can yield nano- and micro-size carbon particles with distinct properties such as a high energetic value, a high chemical and thermal stability, and a moderately high surface area and adsorption capacity (Hu et al. 2008; M.-M. Titirici et al. 2007; Wang et al. 2001).

In 2010, a company named AVA-CO2 made the first step towards a commercial application of HTC, by opening up the world‘s first industrial-scale HTC demonstration plant in Karlsruhe, Germany and 2014, the world's first plant for commercial 5-hydroxymethyl furfural (HMF) production was commissioned in Muttenz, Switzerland (AVA-CO2 2015).

Other companies in this field are Grenol GmbH (Wühlfrath, Germany), TerraNova (Kaiserslautern, Germany), REVATEC GmbH (Emslan, Germany), SunCoal (Brandenburg, Germany), carbonSolutions (Teltow, Germany), Loritus GmbH (München, Germany) and Antaco (Guildford, UK).

1.2 Description of the Process and Process Parameters

As opposed to processes such as torrefaction or gasification, HTC uses hot water at an elevated pressure to carbonise biomass, therefore HTC is also referred as wet pyrolysis. This process is used to carbonise different feed materials under subcritical conditions in order to gain products with higher carbon contents. The product properties, their relative proportions in the gas, liquid and solid phases and the energy requirements depend upon the input material and the process conditions (Libra et al. 2011). In contrast to standard high temperature carbonisation processes, the hydrothermal carbonisation is an exothermic process and energetically more favourable (Funke & Ziegler 2010; M.-M. Titirici et al. 2007). Besides the process temperature, there are other factors which influence the hydrothermal carbonisation including, residence time, pressure, pH and the use of catalysers. As mentioned above, the advantage of HTC is that it can convert wet feed materials into carbonaceous solids at

relatively high yields without the need of an energy-intensive drying before or during the process. This opens up the field of potential feedstocks to a variety of non-traditional sources such as wet animal manures, human waste, sewage sludge, municipal solid waste, biogas slurries, as well as aquaculture and algal residues (Libra et al. 2011).

1.3 Applications for Hydrochars

The HTC process can generate a variety of sustainable carbonaceous materials for a wide range of applications, those can be divided into two main categories large scale applications with mostly low value products and small scale applications with mostly high value products. This categorisation helps to distinguish between processes which use bulk materials for conversation and are feasible in higher scales and processes which use well defined precursors to produced novel materials with specific technical functionalities. It's important to note, that so called "small scale applications" do not necessarily need to be processes at small scale.

1.3.1 Large Scale Applications

1.3.1.1 Energy Vector

The most prominent approach is focused on the possibility to recover energy from the biomass, through the hydrothermal carbonisation. Reported higher heating values ranging from 13.8 MJ/kg for carbonised municipal solid dry wastes (Hwang et al. 2012) to 36 MJ/kg for HTC of anaerobically digested maize silage (Mumme et al. 2011). Typical heating values from HTC of lignocellulosic biomasses are about 30 MJ/kg, which is about 40% higher than that of the starting biomass precursor and these values are similar to those of coals. It has been reported by many authors (Libra et al. 2011; Kang et al. 2012; Hwang et al. 2012; Xiao et al. 2012; Mumme et al. 2011; Heilmann et al. 2011; Lu et al. 2011; Liu & Balasubramanian 2012) that HTC is an effective process for the production of a solid fuel which could be used together with or in substitution of coal. In fact, the HTC process is able to produce a practically homogeneous hydrochar, suitable for the co-combustion with coal, with low moisture content, regular shape and high bulk density (Lu et al. 2011). With respect to the combustion of the raw biomass, the hydrochar has advantages such as higher ignition temperatures, higher combustion temperature regions and higher weight loss rates (Liu & Balasubramanian 2012). Nevertheless, biomass co-fired in coal-fired power stations does not qualify for renewable energy feed-in tariffs in most European countries, therefore the HTC coal most probably has to compete against fossil coal and carbon certificates (Stemann et al. 2013).

Other possible problems that start-up companies in this field face are high investment costs, lack of long-term continuous operation data and the remaining uncertainty with regard to HTC performance and variable costs.

1.3.1.2 Soil Amendment and CO_2-Sequestration

Another promising application is the use of hydrochar as soil amendment and for carbon sequestration. As a matter of fact, anthropogenic CO_2 emissions can be mitigated by converting biomass into charcoal. When converting waste biomass into hydrochar, the carbon bound in the parent biomass will be no longer liberated via microbial decomposition of the biomass residue but bound to the final solid carbonaceous structure. This represents an efficient way of taking the CO_2 out of the carbon cycle and thus offers a solution for reducing greenhouse gas emission. The concept of hydrochar as an approach to carbon sequestration, as well as increasing soil fertility and raising agricultural productivity has received increasing attention over the past few years. Because of the high carbon content and chemical and physical characteristics of hydrochar, a more direct use of the hydrochar for soil melioration and for long term carbon storage has been suggested (Lehmann 2007). For this purpose, the behaviour and characteristics of hydrochar have been investigated by some authors (Libra et al. 2011; Mumme et al. 2011; Becker et al. 2013; Wiedner et al. 2013), focusing on how the HTC process could affect parameters such as the stability of hydrochar in soils, the presence within the hydrochar of hazardous or inhibitor chemicals and greenhouse gas emissions from soils containing hydrochar. In comparison to the biochar (obtained through pyrolysis), the hydrochar has less aromatic structures and higher percentage of labile carbon species, which implies a lower stability when applied to soils (Wiedner et al. 2013). Regarding the chemical composition, chars from hydrothermal carbonisation of waste feedstocks retain high levels of calcium, potassium and phosphorous. However under hydrothermal conditions, dissolution of water-soluble minerals can be significant (Libra et al. 2011). Additional research on process combinations to recover nutrients from the liquid phase is needed and the availability of these nutrients for plants has to be considered. Besides potentially benign effect on soil quality, a recent study was focusing on the potential presence of harmful volatile organic compounds (VOCs), present in the inlet feedstock or generated during an HTC process, which can have environmental consequences when hydrochar is applied as soil amendment (Becker et al. 2013).

A common feature, that all large scale application share, is the use of biomass containing waste stream as feedstock. Biomass in general is defined here in terms of source: “the biodegradable fraction of products, waste and residues from biological origin from agriculture (including vegetal and animal substances), forestry and related industries including fisheries and aquaculture, as well as the biodegradable fraction of industrial and municipal waste” (Berge et al. 2011). These feedstocks usually require some degree of management, treatment and/or processing to ensure an environmentally safe utilisation. Many of these streams (e.g., human waste and municipal waste) have substantial collection and treatment costs associated with them. Hydrothermal carbonisation of biomass has certain advantages when compared with common biological treatment. It generally takes only hours, instead of the days or months required for biological processes (e.g. composting or biological degradation of sludge) permitting a more compact reactor design. Furthermore, some feedstocks are toxic and cannot be converted biochemically, but the high process temperatures of HTC can destroy pathogens and potentially organic contaminants such as pharmaceutically active compounds (Libra et al. 2011).

1.3.2 Small Scale Applications

Hydrothermal carbonisation changes the surface, structure and chemical composition of the feed materials. This can be used to modify the surface area and porosity of materials for specific applications, typically enhancing the adsorption capacity/selectivity or catalytic activity. In contrast to large scale HTC applications, in this field pure carbohydrates (e.g. fructose, glucose, sucrose) are used as precursors, mostly because they are easy dissolvable in water. So called porous carbon materials are becoming of increasing interest in the developing application fields of energy storage e.g. electrodes for Li-ion batteries or supercapacitors (Su & Centi 2013), fuel cells e.g., novel catalysts or catalyst supports for the oxygen reduction reaction (Othman et al. 2012; Joo et al. 2009) and chromatography technologies (Hanai 2003; Knox et al. 1986). However these modifications with HTC at low temperatures (180–250 °C) are limited and hydrochars do usually not offer desired surface area and pore volumes, thereby inhibiting their use in the aforementioned application fields. Therefore several synthetic routes to introduce well-defined porosity into hydrothermal carbons have been developed. Most techniques focus on introducing porosity into carbon materials by either using appropriate nanostructured silica materials as sacrificial templates

("hard templating") or via the self-assembly of block copolymers and suitable aromatic carbon precursors ("soft templating"). But attention is also be given to the utilization of naturally occurring biocomposites (e.g., crustacean shells) and their use in the preparation of porous carbonaceous materials. The hydrothermal process has clear advantages when compared to pyrolysis and other classical carbonisation methods since it takes place in the aqueous phase and thus can, be easily combined with classical templating procedures (Titirici 2013). Additionally, the materials surface can be further modified to extend the range of possible applications and tune material properties. Compared to carbon materials derived from conventional carbonisation procedures, HTC-derived materials offer polar functionalities on their surfaces, allowing further modification to be performed (Titirici & Antonietti 2010). The introduction of, for example, sulphur or nitrogen into a carbon material can result in improved electrical conductivity, material stability, and catalytic performance due to an increased number of active sites (Wohlgemuth et al. 2012; Terrones et al. 2002). Compared to current synthetic procedures for carbon materials, the hydrothermal process is less energy consuming, only water as solvent is needed and non-fossil-based precursors are used.

1.4 Reaction Mechanisms of HTC

The HTC process includes several reaction mechanisms, such as hydrolysis, dehydration, decarboxylation, polymerization and aromatization, although the detailed reaction pathways have only been well characterized for a few types of organic materials, such as glucose and cellulose. Since the substrate for these chemical reaction are often embedded in biomass matrices, the reaction rates are most probably hindered by diffusion. The mentioned chemical reactions as well as the macro kinetic mechanisms are described here in detail:

1.4.1 Hydrolysis

Hydrolytic reactions lead to the cleavage of mainly ester and ether bonds of the macromolecules by addition of water yielding a wide range of products including (oligo-) saccharides of cellulose and phenolic fragments of lignin. The resulting reaction network is most probably very complex since already the hydrolysis of D-fructose shows a complex pathway, which is a specified substance in contrast to biomass (Antal et al. 1990). The hydrolysis reactions are possible due to the relatively high values of the ionic product of H^+ and OH^- generated by water autoionisation under hydrothermal conditions (Garrote et al. 1999). Besides other degradation mechanisms mentioned below, the resulting fragments are being further hydrolysed which leads to the formation of 5-HMF and organic

acids (e.g., acetic, lactic, propenoic, levulinic, and formic acids) which rapidly decrease the pH (Kuster 1990). In Figure 2 the main reaction pathways of the biomass monomers glucose and fructose are shown.

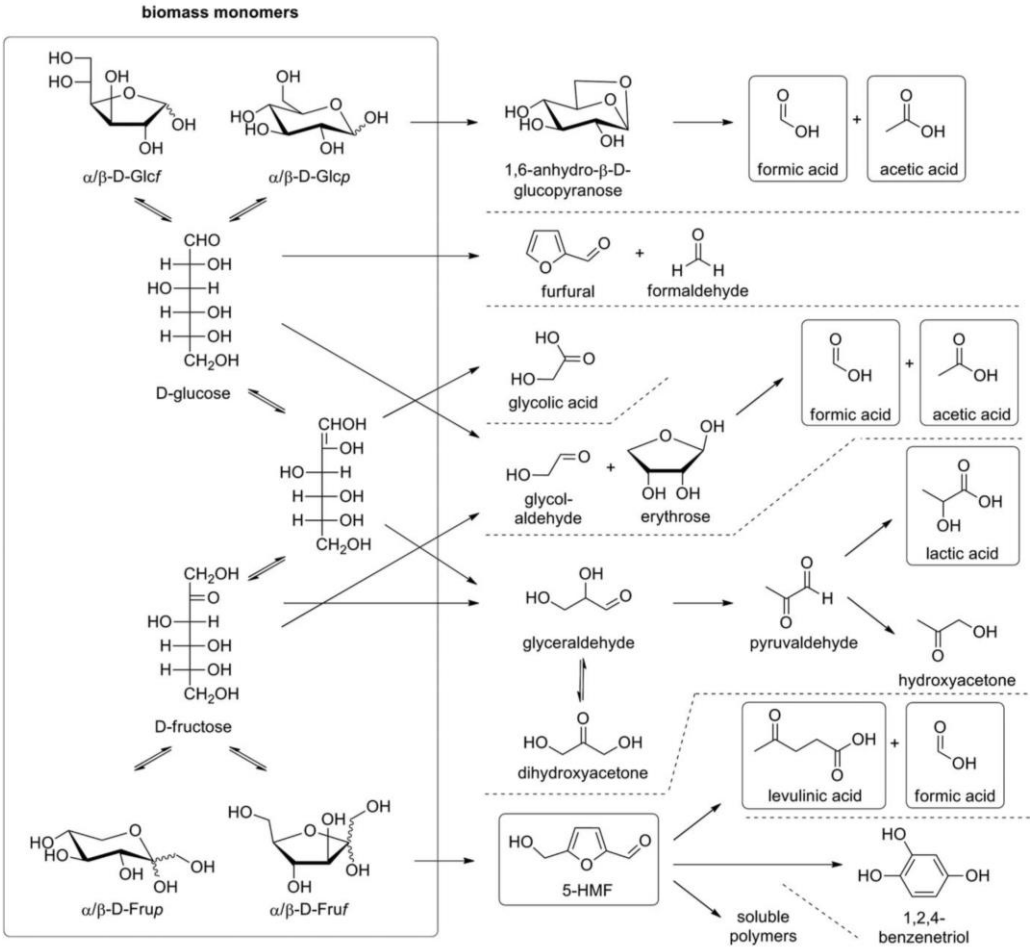

Figure 2. Main reaction pathways of glucose and fructose in subcritical water. Glcp=glucopyranose, Glcf=glucofuranose, Frup=fructopyranose, Fruf=fructofuranose, 5-HMF=5-(hydroxymethyl)furfural (Möller et al. 2011).

It is known, that hemicellulose is already hydrolysed under hydrothermal conditions at around 180°C, cellulose is being hydrolysed significantly above approximately 200°C and degradation of lignin is most likely realisable above 260°C due to its high amount of ether bonds (Zhang et al. 2008). Ongoing hydrolysis also yields also highly reactive fragments which quickly form precipitates by condensation reactions. These interactions between the different biomass components and its fragments cannot be avoided. The effect of such interactions on hydrolysis is largely unknown, but it has been reported, that hemicellulose fragments interact with lignin and either enhance the solubility of its aromatic structures

(Bobleter & Binder 1980) or form an oligomer which is usually stable under hydrothermal conditions (Mok & Antal 1992).

1.4.2 Dehydration

Dehydration during hydrothermal carbonisation can cover both chemical reactions and physical processes, which remove water from the biomass without changing its chemical constitution (Funke & Ziegler 2010). This reaction is also referred as dewatering. Chemical dehydration significantly carbonises biomass by lowering the H/C and O/C ratios as can be seen in Figure 3. Early experiments with oil discovered that cellulose starts decomposing by pure dehydration according to

$$2(C_6H_{10}O_5)_n \leftrightarrow (C_{12}H_{10}O_5)_n + 5H_2O$$

Equation 1. Dehydration of oil (adopted from Funke and Ziegler 2010)

During common HTC, the rate of dehydration is assumed to be much higher than decarboxylation. This is supported by the finding, that significant decarboxylation does only appears after that specific amount of water is formed by dehydration (Bergius 1928). In addition, experimental results under hydrothermal conditions show that at low reaction severity, dehydration can be achieved without significant decarboxylation (Titirici et al. 2007) In general, dehydration is explained by elimination of hydroxyl groups, which can occur with nearly any carboxylic group when heated to a certain temperature (Sykes 1973). Detailed studies exist for the case of hydrothermal dehydration of glucose to HMF or 1,6-anhydroglucose (Titirici et al. 2007) and in case of lignin, the dehydroxilation of catechol is mentioned as well as the possible formation of water during the cleavage of phenolic and alcohol groups above 150°C and 200°C, respectively (Murray & Evans 1972; Hirschon et al. 1991). Another cause for water removal during hydrothermal carbonisation may be due to the condensation of fragments, which is discussed below.

1.4.3 Decarboxylation

The hydrothermal carbonisation reaction includes partial elimination of carboxyl groups (Parshetti et al. 2013; Berge et al. 2011; He et al. 2013; Hoekman et al. 2011). The degradation of carboxyl and carbonyl groups occur rapidly above 150°C, yielding CO_2 and CO, respectively (Murray & Evans 1972). Detailed reaction mechanisms for these decarboxylation reactions are

largely unknown, including the effect of the presence of water (Peterson et al. 2008). It can be concluded that more CO_2 is being formed than can be explained by elimination of carboxyl groups (Funke & Ziegler 2010). Therefore other mechanisms must be involved, such as the formation of formic acid which is coupled with the degradation of cellulose and then decomposes under hydrothermal conditions to yield primarily CO_2 and H_2O (McCollom et al. 1999). Other possible sources may be the formation of CO_2 during condensation reactions which are explained below.

1.4.4 Aromatisation and Polymerisation

Since it is known that cellulose and other carbohydrates are able to form aromatic structures under hydrothermal conditions (Luijkx 1994), it has to be considered, that aromatisation reaction also lower atomic O/C ratios. At the same time, aromatisation reaction increase with temperature (Falco et al. 2011), therefore it is assumed, that around 180°C aromatisation reactions play a minor role in the overall carbonisation reaction.

Also polymerisation reactions occur during HTC, where reactive catalytic products of hydrolysis undergo condensation and polymerisation reactions, specifically aldol condensation (Funke & Ziegler 2010). These reactions are important for the chemical formation of carbonaceous spheres (Yao et al. 2007). Yao et al. (2007) provided experimental evidence to suggest that the formation of carbonaceous spheres from a fructose solution occurred by polymerisation of intermediate HMF compounds. Furthermore Baccile et al. (2009) confirmed that those carbon spheres derived from a range of carbohydrates are composed of furanic rings instead of in graphene-based structures, thereby supporting the chemical route proposed by Yao et al. (2007).

1.4.5 Van Krevelen Diagram

A Van Krevelen diagram shows H/C and O/C atomic ratios, which is useful for representing the conversion of carbohydrate material to carbon-rich material (see Figure 3). This diagram offers a clear insight into the chemical transformations of the carbon rich material, which are demethanation (production of methane), dehydration (production of water) and decarboxylation (production of carbonyls including carboxylic acids), taking place during the process (Fuertes et al. 2010).

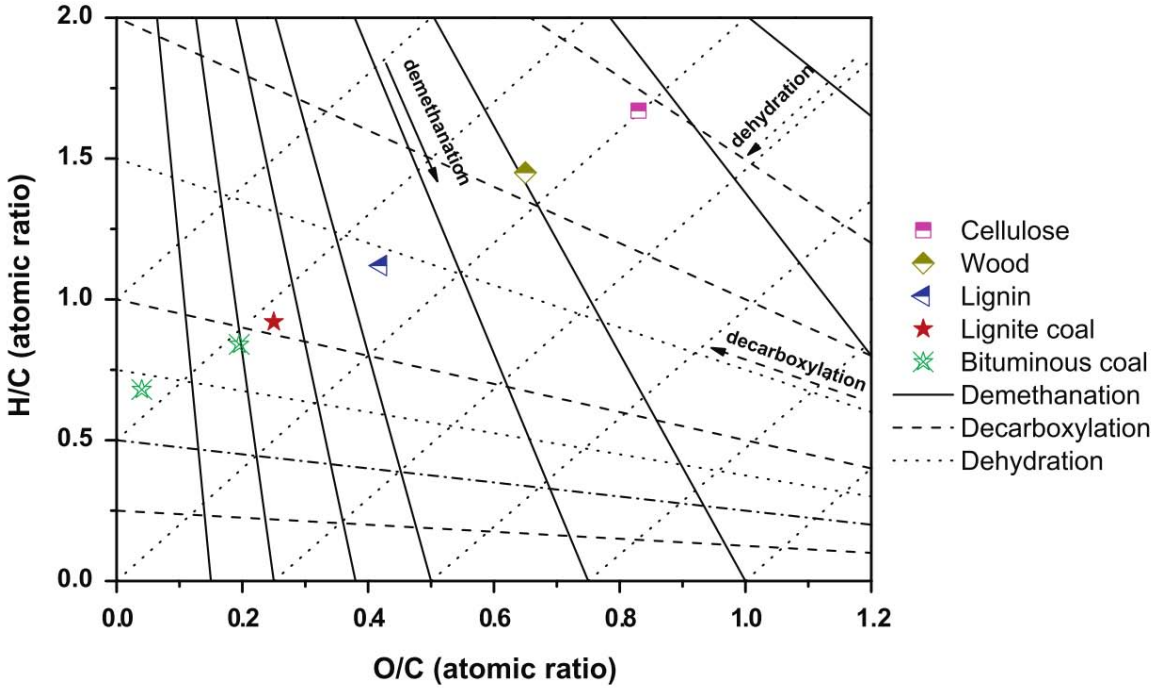

Figure 3 Atomic H/C versus O/C ratios (Van Krevelen diagram) of feedstocks and chars resulting from carbonisation. The lines represent demethanation, dehydration, and decarboxylation pathways (Xiao et al. 2012).

Following the reaction pathways of biomass to hydrochars, it is obvious that dehydration and decarboxylation were the essential reaction pathways in HTC while the demethanation pathway was negligible (He et al. 2013). Therefore it can be assumed, that the O/C and H/C ratios are proportional to the degree of carbonisation. It is important to note, that this study is only focusing on O/C atomic ratios, since hydrogen cannot be determined by EDX analysis. Nevertheless is known that organic feed materials do follow a distinct path in the Van Krevelen diagram during HTC, by lowering their O/C and H/C atomic ratios.

1.4.6 Macrokinetics and Diffusion

Hydrothermal carbonisation of lignocellulosic biomass and related reactions have been suggested by many authors to be influenced by diffusion (Reza et al. 2013; Garrote et al. 1999; Hirschon et al. 1991). In a kinetic study of the polysaccharide hydrolysis by the catalytic action of hydronium ions the following sequential steps where proposed by Fengel & Wegener, 1984 and visualised in Figure 4 (D. Fengel and G. Wegener 1984):

i) diffusion of the catalyst in the polysaccharide heterogeneous matrix;

ii) protonation of the heterocyclic ether;

iii) breaking of the ether bond with generation of a carbonium ion and a new polymer, oligomer or monomer (depending on the position of the broken bond on the polymer chain);

iv) regeneration of the hydronium ion by hydrolysis of water, with the generation of a saccharide having a polymerization degree dependent on the position of the broken bond;

v) diffusion of the reaction products through the solid matrix and in the liquid phase.

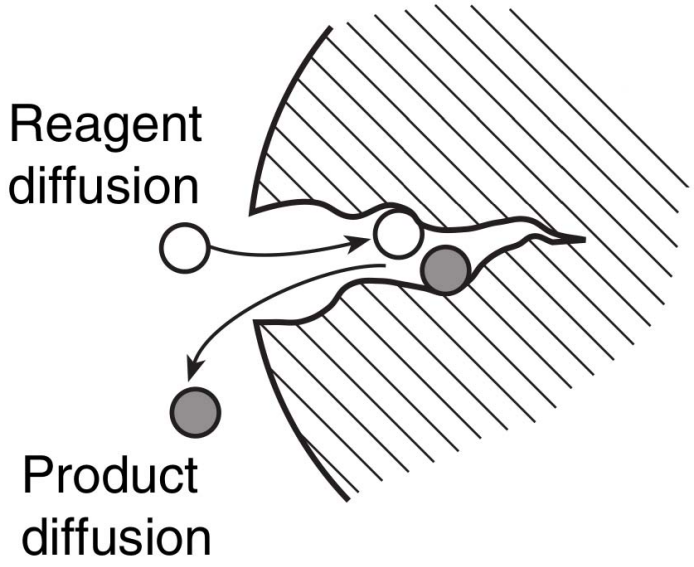

Figure 4. Diffusion controlled reaction: a reagent slowly diffuses into the pores of a catalyst pellet, reacting all along the way.

Because of this behaviour, reaction occurring in the pore is compromised by diffusion. In the case of hydrothermal carbonisation, the diffusion of monomers (fructose, glucose, HMF) to the surface of the particle are assumed to be the rate limiting step. Therefore the effectiveness factor (η) is used, which was introduced by Thiele and it describes the ratio of reaction with mass transfer to that without any limitations of mass transfer. The effectiveness factor can be calculated from the Thiele module, which describes the concentration gradient of a reacting agent in a cylindrical pore:

$$\eta = \frac{3}{\Phi} * \left(\frac{1}{\tanh(\Phi)} - \frac{1}{\Phi} \right)$$

Equation 2. Effectiveness factor for a first order irreversible reaction, Φ Thiele module.

The Thiele module is a dimensionless number and it can be regarded as a measure for the ratio of the reaction rate (k) to the rate of diffusion (D_{eff}):

$$\Phi = X_0 \sqrt{\frac{k}{D_{eff}}}$$

Equation 3. Thiele module for a first order reaction.

In order to generalize the equation for different geometric shaped catalysers, the characteristic geometric length is used:

$$X_0 = \frac{V_P}{A_P}$$

Equation 4. Characteristic geometric length, V_P volume of the particle and A_P area of the Particle.

This model was first introduced by E. W. Thiele in 1939, where it was used to describe heterogenic reactions (gas/solid and liquid/solid) occurring in porous catalytic pellets (Thiele 1939). Nowadays it is used in many different fields to describe the following behaviours, including gasification of coal particles (Bell et al. 2011), enzymatic reactions in membranes (Bisswanger 2008), the biological transport of oxygen through cells (Najafpour 2007) and pharmaceutical drug delivery systems (Polishchuk & Zaikov 1997). One advantage of using the effectiveness factor, is the ability to calculate the intrinsic reaction rate from the observed reaction rate as follows:

$$r_{observed} = \eta * r_{intrinsic}$$

Equation 5: Effectiveness factor & reaction rates (Holder 2008)

The relationship between the Thiele module and the effectiveness factor for a spherical particle is visualised in Figure 5. It shows, that as $\Phi \rightarrow 0$ the effectiveness factor $\eta \rightarrow 1$ and as $\Phi \rightarrow \infty$, the effectiveness factor η becomes inversely proportional to Φ. This means as $\Phi \rightarrow \infty$, $\eta \approx \frac{3}{\Phi}$ because $\tanh(\Phi) = 0$ at $\Phi = 0$ and $\tanh(\Phi) \rightarrow 1$ as $\Phi \rightarrow \infty$ (Speight & Ozum 2001). In other words, if $\eta \rightarrow 1$ and $\Phi \rightarrow 0$, the observed reaction rate is equal to the intrinsic reaction rate which can be achieved, by pulverizing the material. On the other hand,

with increasing particle size the Thiele module is increasing and reducing the observed reaction rate by the factor η.

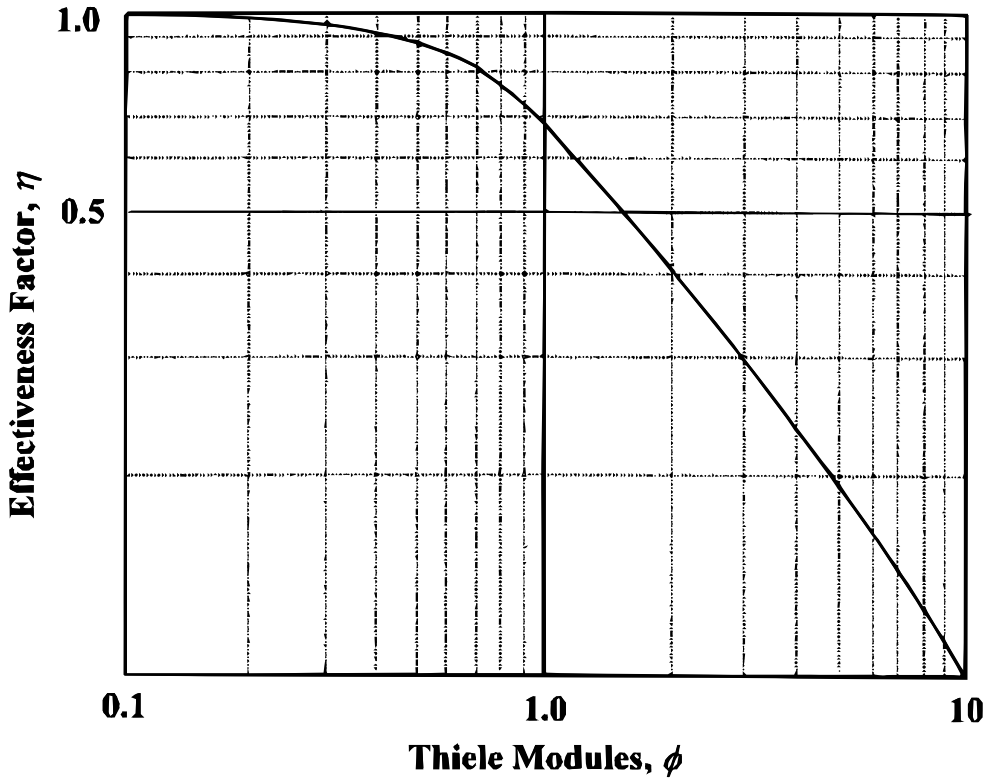

Figure 5. Effectiveness factor as a function of Thiele module for a spherical particle reacting with a fluid. (Speight & Ozum 2001)

1.5 Motivation

Hydrothermal carbonisation of lignocellulosic materials is highly complex and not yet fully understood (Funke & Ziegler 2010; Kang et al. 2012). Deficits in knowledge especially regard the use of biomass, as the vast majority of reported experiments dealt with basic organic compounds such as glucose, cellulose, and lignin. In order to make hydrochar production economically feasible and eco-friendly, the use of biomass and in particular organic wastes seems inevitable (Mumme et al. 2011). At present, the residence time cannot be limited to a meaningful range because reaction rates are largely unknown but typical published experimental times varied between 1 and 72h (Funke & Ziegler 2010). Furthermore, particle sizes of HTC feedstock is assumed to play a minor importance since HTC takes place in subcritical water, which offers a good heat transfer to the inside of a particle (Titirici 2013). On the other hand, HTC reactions is assumed to occur within the pores of the biomass and

thus, hot water must enter the pores, while at the same time, the aqueous products must leave the pores - this diffusion dependent reaction could be a rate limiting step (Reza et al. 2013).

1.6 Aims

In this study, different feed materials and their solid products of HTC were analysed with a scanning electron microscope in order to find a proper material for a micro kinetic analysis. Thereby the Thiele module based on the measured molar O/C profiles was calculated. The resulting Thiele modules together with a structural analysis, should give insight into the heterogenic reaction occurring in the biomass particles under hydrothermal conditions. Furthermore, these findings should contribute to the understanding of the hydrothermal carbonisation and degradation reactions of biomass and aid the development and scale-up and optimisation of HTC-processes.

2. Material and Methods

2.1 HTC Batch Reactor

In this study a 1.5 litre tubular vessel made out of stainless steel with a diameter of 12.8 cm was used to carbonise different organic materials (see Figure 6).

Figure 6. Opened tubular HTC reactor filled with bamboo sticks and water.

The top of the vessel is closed by a circular lid with 12 screws and an O-ring. The reactor is equipped with a temperature sensor (PT100), pressure sensor, overpressure valve (25 bar) and a manual valve for releasing gases. During the process, the reactor is placed in a metal box which is insulated with glass wool. The process is temperature controlled by an on-off controller from a PLC provided by B&R®.

In this study, a temperature of 180° C was selected and different residence times (1, 6 and 12 hours) were applied. In Figure 7, a representative temperature and pressure profile (heating and holding phase) from a 6 hour experiment obtained from the HTC reactor is shown. The process can be divided into the following steps:

a) Heating phase: it takes around 45 minutes to reach the desired set point of 180°C
b) Holding phase: is equivalent to residence time - the temperature is kept constant.
c) Cooling phase: Heating device is switched off and insulation is removed (not shown in Figure 7).
d) Pressure release: Before opening the vessel, the inner pressure is released by opening the valve (not shown in Figure 7).

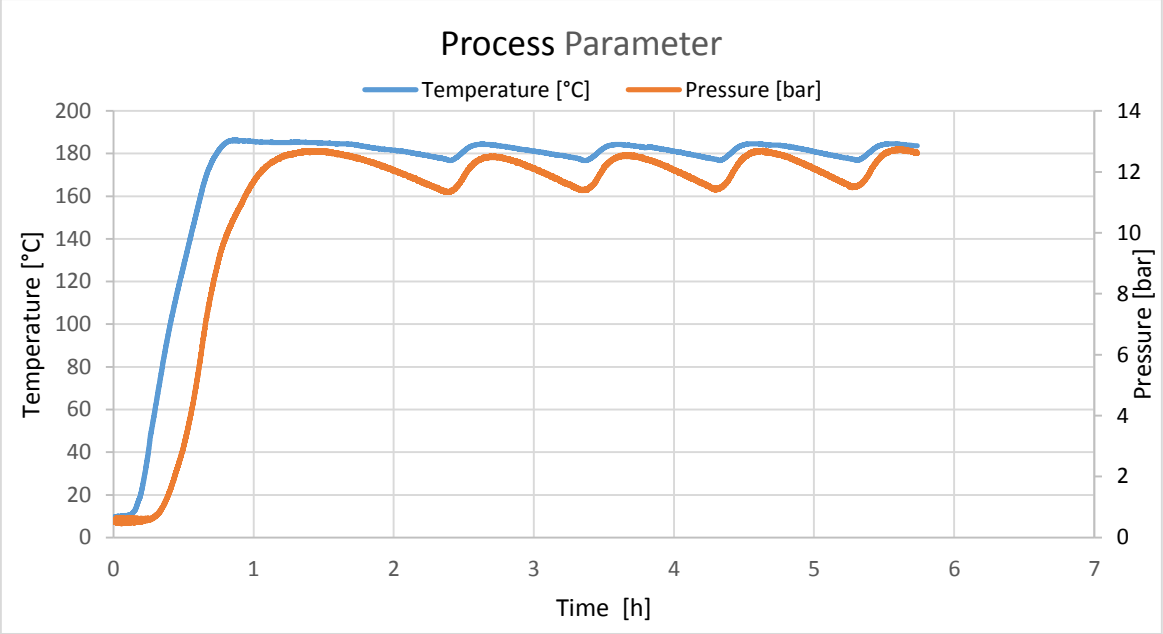

Figure 7 - Representative temperature and pressure profile obtained from a HTC process by using the tubular reactor: heating and holding phase.

It is important to note, that the residence time starts after achieving 180°C and ends with the cooling phase. This has especially to be considered, when results are compared with data from other reactors and processes.

Whit the described HTC reactor, the following experiments were performed:

feed materials	experiments	SEM analysis	EDX analysis
pistachio shells	1 hour	✓	n=3
	6 hours	✓	n=3
	12 hours	✓	n=3
bamboo sticks	2 hours	✓	n=3
fir needles	1 hour	✓	not possible
biogas slurry	1 hour	low image quality	not possible

Table 1. Overview of performed HTC experiments and SEM-EDX analysis.

2.2 Feed Materials

Within this thesis, the following feed materials were used:

feed materials	C [%w]	H [%w]	N [%w]	S [%w]	Source
bamboo sticks	46.80%	6.38%	0.22%	-	Rousset et al. 2011
pistachio shells	44.71%	6.31%	0.09%	0.02%	Madner 2014
fir needles	46.92%	6.02%	1.74%	0.06%	Madner 2014
biogas slurry	34.55%	4.80%	3.34%	1.19%	Stutzenstein 2015

Table 2. Overview of HTC feed materials with chemical compositions (C, H, N and S).

Besides biogas slurry, all other feed materials where dry materials with a water content probably lower than 10 wt. %. The reason for that was the fundamental approach to investigate O/C concentration profiles of biomass particles under hydrothermal conditions – which was only possible with dry materials (see Chapter 2.3.3).

2.2.1 Bamboo Sticks:

Bamboo is the common term for a broad group of woody grasses (family Poaceae, subfamily Bambusoideae) ranging from 100 mm to 40 m in height and it encompasses 1250 species within 75 genera (Schneider et al. 2011). Bamboo is known as a durable material, which has an average hardness of 0,44 GPa (Zou et al. 2009). Chemical analysis showed that bamboo (*Bambusa vulgaris*) contains lignin 27.22 wt.%, cellulose 46.08 wt.% and hemicelluloses 69.94 wt.% (Rousset et al. 2011). Even though bamboo is distributed mostly in the tropics, it has several interesting aspects for the HTC. It is a fast-growing plant that can grow on slopes and in an environment where cultivation of wood is not possible (Vogtländer et al. 2010). Average water content values are 10 wt.% at harvest and 3 wt.% after drying (Scurlock et al. 2000). Another important aspect is its homogenous consistency and shape with a characteristic surface topography which is essential for further analysis with SEM-EDX.

2.2.2 Fir Needles

In this study, fir needles were selected as a representative local available biomass. Across Austria, a total of 194 natural forest reserves covering an overall area of approximately 8,550 hectares have been established and 66.8 % of that area are coniferous woods (Kiessling et al. 2009), which are a potential source for biomass. Needles from coniferous trees are known to contain, besides cellulose and hemicelluloses, up to 35% lignin, together with smaller amounts

of terpenes, oils and waxes (M. M. Titirici et al. 2007). Related to the methodology of this study it was important to select precursors which offer a characteristic surface topography. Chemical analysis from previous studies showed, that fir needles have the following elemental composition (%w) 46.92% carbon, 6.02% hydrogen, 1.74% nitrogen and 0.06% sulphur (Madner 2014).

2.2.3 Pistachio Shells

Pistachio shells were selected as a representative hard biomass since the average bulk density of this material was found to be 750 kg/m3 (Apaydin-Varol et al. 2007) and a hardness of 26.3 HRC (Lua et al. 2004) which correlates to 0.86 GPa. The main components of all biomass materials are cellulose, hemicellulose and lignin (Bridgwater & Grassi 1991). Experiments showed that pistachio shells contain 15.2% cellulose, 38.5% hemicellulose, 29.4% lignin, and 17.0% extractives (Salgado et al. 2012). Pistachio is cultivated mostly in Iran, The United States, Turkey, China and Syria; total pistachio world production has reached about 1,005,433 Mt in 2012 which is nearly twice as much since 2009 (FAOSTAT 2012). Chemical analysis from previous studies showed, that the pistachio shells used in this study have the following elemental composition (%w) 44.71% carbon, 6.31% hydrogen, 0.09% nitrogen and 0.02% sulphur (Madner 2014).

2.2.4 Biogas Slurry

Biogas slurry is often referred as a precursor with high potentials for HTC since, it typically shows a high moisture content, a poor dewaterability and high concentrations of carbon and nutrients such as nitrogen and phosphorus (He et al. 2013; Mumme et al. 2011). In addition, it bears the potential risk of high greenhouse gas emissions (Møller et al. 2009). These characteristics make it an interesting feedstock for HTC. The product is meant to be used as soil amendment which promises various benefits such as improved water holding capacity and long-term storage of carbon branched off the biomass cycle that may lead to an overall negative greenhouse gas balance (Becker et al. 2013).

2.3 Elemental Analysis and Surface Analysis

2.3.1 SEM Principles

A scanning electron microscope consists of an electron gun, electron optical column, specimen chamber, detectors and a vacuum system. The analytical principle relies on creating a primary electron beam which is focused on the specimen, thereby certain interactions occur (as can be seen in Figure 8) and a signal in the form of secondary electrons (SE) and backscattered secondary electrons (BSE) is generated. These electrons are captured by a SE/BSE detector and converted into an electrical signal, then an intensity value is generated. In order to obtain an image, the beam is scanned in a rectangular raster over the specimen (line-by-line) and the measurements are taken point-by-point and simultaneously displayed on a monitor. So called SEM micrographs offer a large depth of field yielding a characteristic three-dimensional appearance useful for understanding the surface structure of a sample.

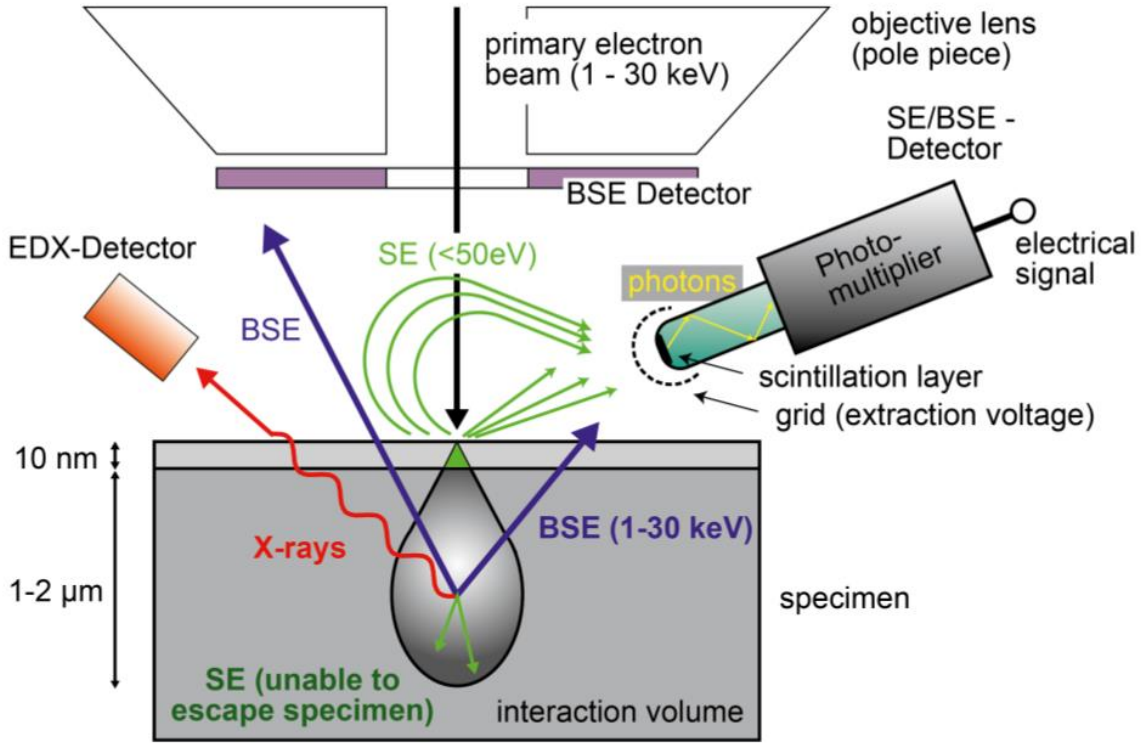

Figure 8. Electron - specimen interactions (Pum 2015)

Since the resolving power of a microscope is ultimately limited by the wavelength of the electromagnetic light, in high resolution microscopy an electron beam (transmission electron microscope and SEM) is used. Accelerated electron in vacuum have a similar behaviour to light. They are traveling in straight lines and have wavelike properties with a wavelength that

is about 100.000 times shorter than that of visible light. Furthermore, it was found that electric and magnetic fields could be used to shape the paths followed by electrons similar to the way glass lenses are used to bend and focus visible light. In 1931 Ernst Ruska at the University of Berlin combined these characteristics and built the first transmission electron microscope (TEM). For this and subsequent work on the subject, he was awarded the Nobel Prize for Physics in 1986. The microscope used in this study, uses a thermionic emitter as an electron source. The so called triode gun consists of a W^{74} (tungsten) filament a LaB_6 (lanthanium hexaboride) crystal, an anode and a Wehnelt cylinder (see Figure 9.).

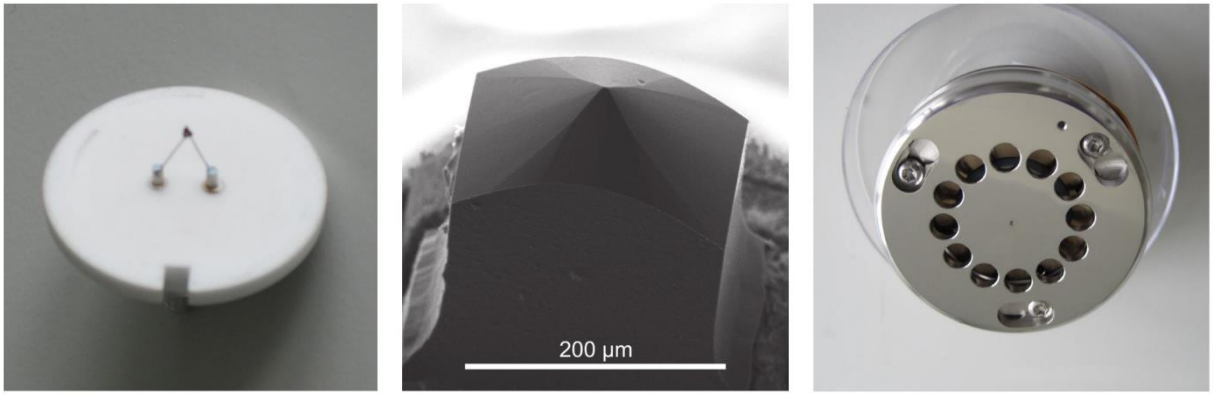

Figure 9. LaB_6 crystal with tungsten hairpin and mounting plat (left), SEM micrograph of LaB_6 crystal (middle) and Wehnelt cylinder (right) (adopted from Pum 2015).

In order to create the electron beam, the tungsten filament is heated to about 2700°C, by applying a high voltage. As can be seen in Figure 10., the filament is surrounded by the Wehnelt cylinder, which is held at a variable potential slightly negative to the filament, in order to hold back the electrons in an electron cloud. From this electron cloud, the electrons are directed through a narrow cross-over (aperture 300µm) down the column, along the optical axis. The Wehnelt cylinder improves the current density and brightness of the beam.

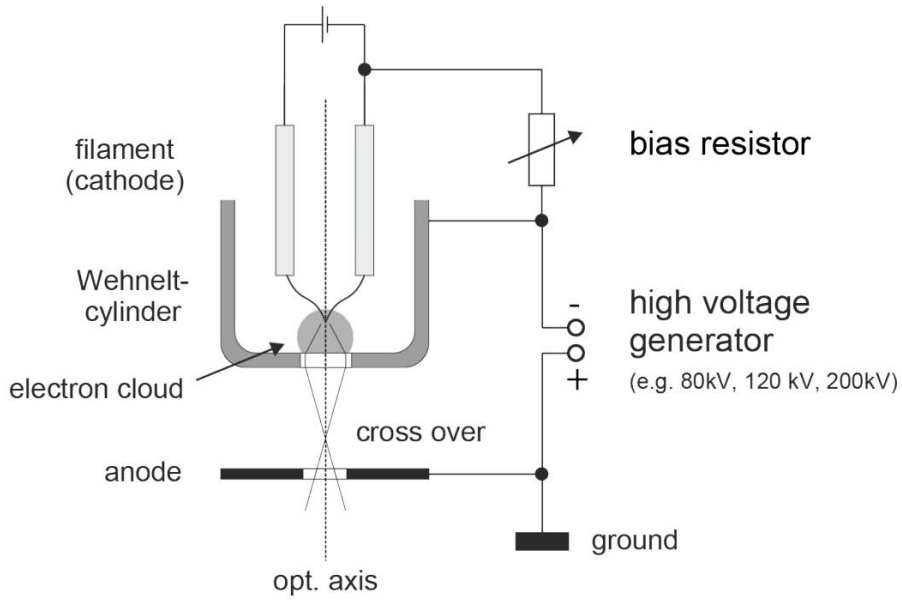

Figure 10. Schematic of the filament system in a scanning electron microscope (Pum 2015).

By applying a high positive potential difference between the filament and the anode, thermally excited electrons are extracted from the electron cloud near the filament and accelerated towards the anode. The anode has a hole in it so that an electron beam emerges and is directed down the column.

2.3.2 EDX Principles

Energy-dispersive X-ray spectroscopy (EDX), is an analytical technique used for the elemental analysis or chemical characterization of a sample. It relies on an interaction of some source of X-ray excitation and a sample. Its characterization capabilities are due in large part to the fundamental principle that each element has a unique atomic structure allowing unique set of peaks on its X-ray emission spectrum. To stimulate the emission of characteristic X-rays from a specimen, the primary electron beam is created a tungsten filament (as described in chapter 2.3.1.) and focused on the surface of the sample. Besides creating SE and BSE (which are essential for creating SEM micrographs), incident electrons may interact with the inner shell electrons of the atoms in the specimen (see Figure 11).

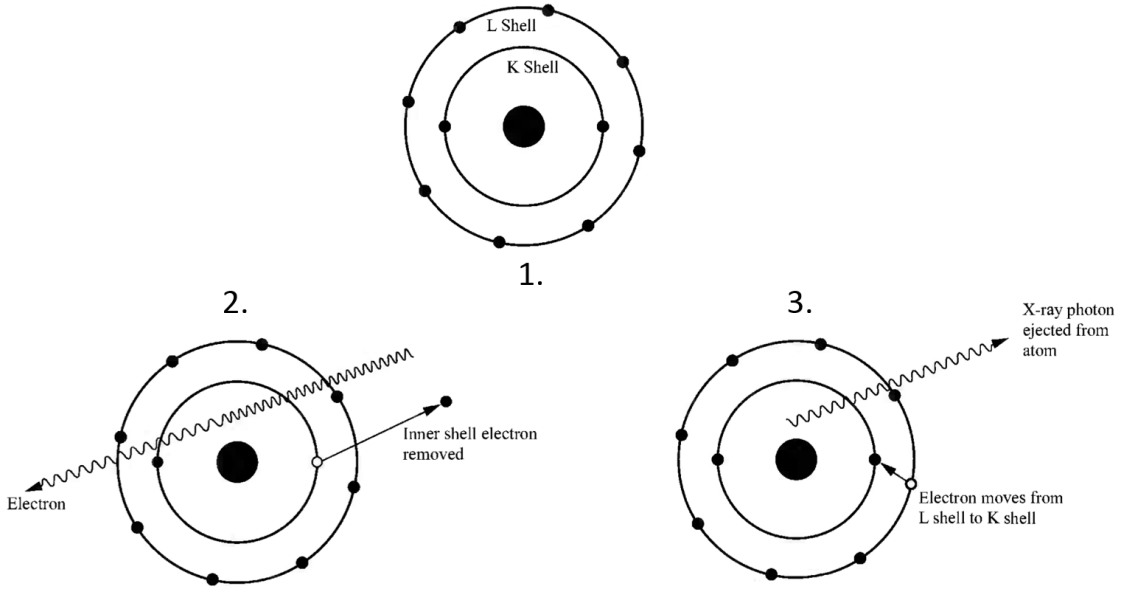

Figure 11. Electron beam interaction on atomic level. (1.) Atom with L-shell and K-shell in native state, (2.) incident electron interaction, (3.) X-ray photon emission (Stevens 2004).

Under certain conditions an incident electron can cause an inner shell electron to be ejected from the target atom, leaving the atom in an energized state. The atom returns to a lower energy state when one of its outer shell electrons fills the space in the lower energy shell. As a cause of this reaction, a photon with the energy equal to that of the difference of the energy levels of the two shells may be produced. The majority of the emitted photons are in the X-ray energy range. In quantum mechanics several characteristics of the energy levels of electrons surrounding an atom and the manner in which electrons can move from one level to another are described. The energy levels of the electron shells are considered to have only certain discrete values and these values are determined mainly by the atomic number of the nucleus. Therefore, the energy levels of the electron shells are different for different elements. Electrons can transit only between certain shells. Since the combination of energy levels of electron shells being different for different elements along with the fact that not all transitions are allowable means that the X-ray photons emitted from atoms are, to a large extent, diagnostic of the atomic number of the target atom and thus, are termed characteristic X-rays (Stevens 2004). The characteristic X-rays are then detected by a Silicon Drift Detector (SDD). This device delivers quantitative information of how many X-rays of any given energy are produced. SSD-EDX has an enhanced peak stability and greatly improved throughput compared to Si(Li)-EDX and it has recently been demonstrated that SDD-EDX can match WDS (wavelength dispersive X-ray spectroscopy) for intensity (Newbury & Ritchie 2013).

2.3.3 Analytical Method for SEM-EDX

In this study a scanning electron microscope (FEI Inspect S50) was used for surface analysis of different feed and product materials. In order to measure the elemental distribution on the surface of the sample, an EDX detector was used. For data interpretation and quantification the FEI software was used, thereby a standardless quantification was performed. By using the low vacuum mode (around 0.75 mbar) no additional sample preparations were needed (e.g. sputter coating or critical point drying).

Since SEM analysis require dry samples (water is evaporating under vacuum), the sample materials (feed materials and hydrochars) were air dried for several days. In case of biogas slurry, an industrial oven was used to dry the material at 110°C for 4-5 hours. The dry samples were cut with a razor blade in the desired shape, then a conductive adhesive “Leit-C” was used to mount the sample onto the aluminium stub. Then the stubs were mounted on the table in the specimen chamber of the microscope and after closing the lid, a vacuum of 0.75 mbar was applied. Images and EDX data were created by using an electron beam of 15kV with a spot size of 4 (dimensionless) and capturing X-rays with an Element Silicon Drift Detector (SSD Apollo, EDAX ®). In Figure 12, a representative EDX spectra obtained from a carbonised bamboo stick is shown.

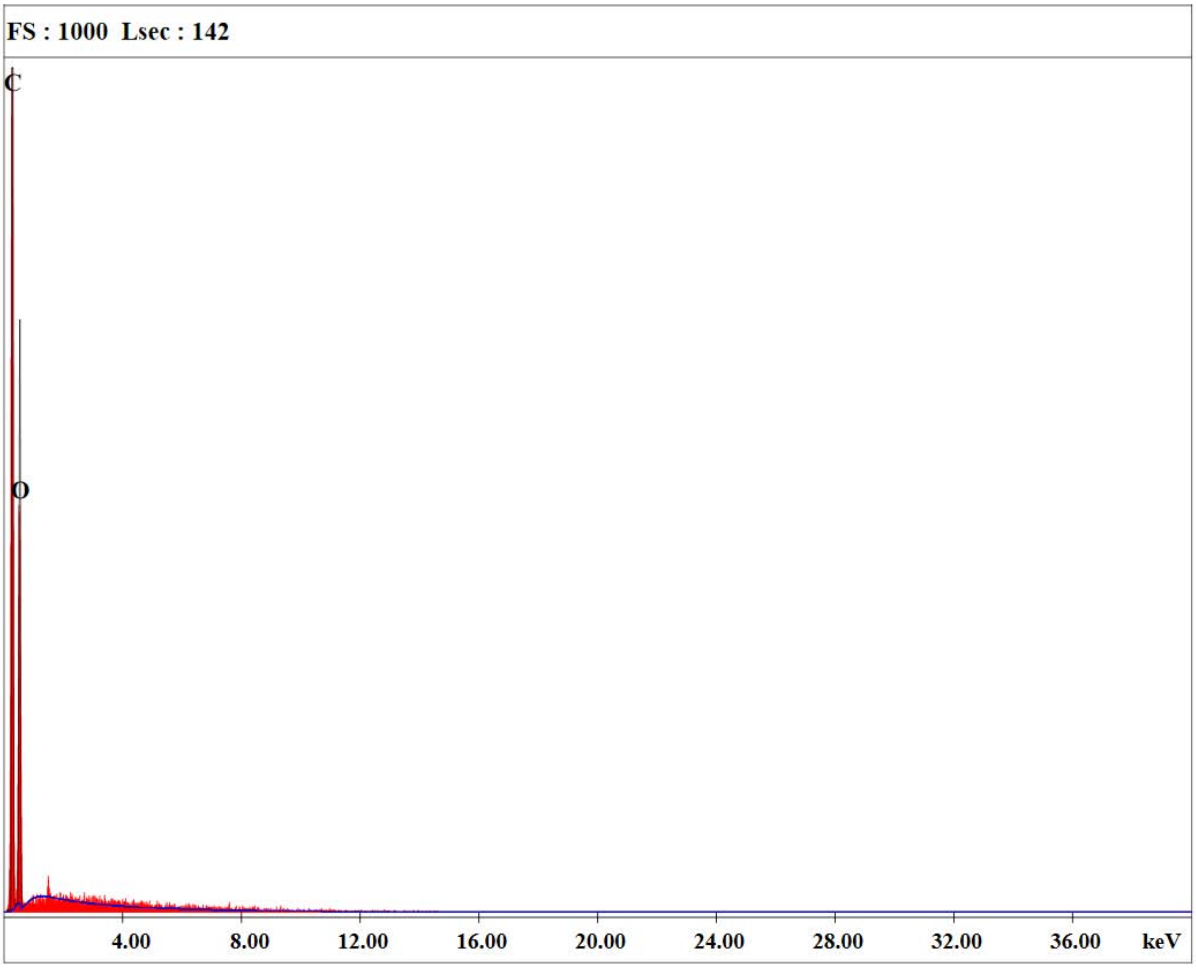

Figure 12. Representative EDX spectra obtained from bamboo hydrochar after 2 hours of residence time.

Typically an EDX spectra shows the signal intensity versus the energy level of the emitted X-rays. As can be seen in Figure 12, only two peaks in the range of 0-38 keV were detected, their energy level corresponds to the K-shells of carbon and oxygen. The advantage of this method, is the ability to measure atomic compositions (qualitative and semi-quantitative) on distinct areas of the sample. In this study it was used to determine O/C molar ratios in selected areas (0.01 mm^2) of from the surface to the centre of particles.

2.3.4 Particle Modelling and Thiele Module

In this chapter it is explained, how the EDX data is normalised and fit to the model of the Thiele module. Thereby, exemplary concentration profiles of different Thiele modules are calculated with the exponential Equation 6 and shown in Figure 13.

$$\frac{C_X}{C_0} = \frac{\cosh\left[\Phi\left(1-\frac{x}{L}\right)\right]}{\cosh(\Phi)}$$

Equation 6: Theoretical, exponential correlation between Concentration, pore length and Thiele module. C_0 = highest concentration (surface), C_X = concentration over the dimensionless pore length, (x/L) = dimensionless pore length.

This theoretical model describes the concentration profile of a reactant over the dimensionless pore length. Since usually, the measurement of the reactant is not possible, Thiele modules are calculated either by varying particle sizes or via the reaction constant (as performed by Reza et al. 2013). In this study, an alternative approach is used, where the O/C atomic ratio is measured, which is assumed to be proportional to the reactants concentration in the pore.

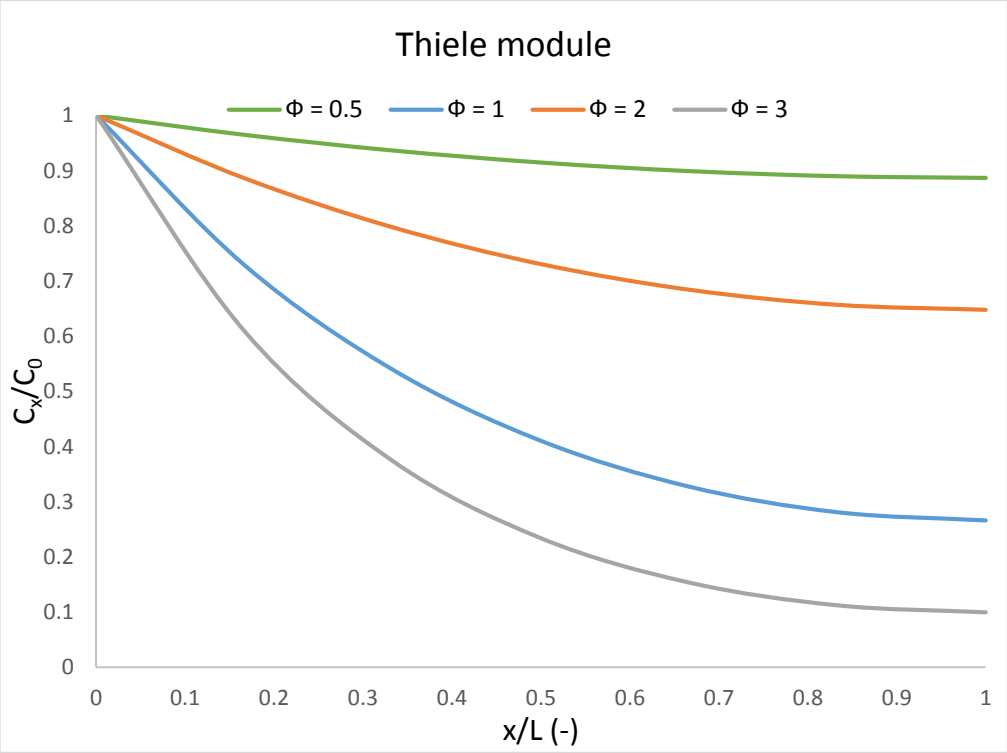

Figure 13: Theoretical model of concentration profiles over dimensionless pore length at different Thiele modules.

It is assumed, that the theoretical model of the Thiele module differs from the EDX experiment because of the following aspects:

- the highest molar O/C concentration is expected to be inside the particle and not on the surface

- it is assumed, that sugar monomers are the product of heterogenic reactions, which have to diffuse out of the pore (analogy to Reza et al. 2013) – this could be a rate limiting step
- The O/C profile is not in steady state, instead, it is lowered over time

Therefore, measured molar O/C ratios had to be normalised in order to fulfill the criteria of the Thiele module plot (Figure 13). The proposed equation for normalising the measured concentrations is shown here:

$$\frac{C_x}{C_0} = \frac{C_{native} - C_{\left(\frac{x}{L}\right)}}{C_{native} - C_s}$$

Equation 7: Normalisation of data. C_S= concentration at the surface, C_{native}= mean concentration of the native feed material, $C_{(X/L)}$ = Concentration over dimensionless pore length.

By subtracting the lowest concentration (C_s) from each point of the profile, the influence of time is removed and at a depth of 0 (-), the normalised concentration ($\frac{C_x}{C_0}$) is 1. In a second step, the Thiele module is then calculated from Equation 6 via least square regression. Thereby, the software “CurveExpert Professional” was used.

3. Results

3.1 Surface Analysis

The following micrographs were obtained from carbonised pistachio shells and native pistachio shells according chapter 2.3.3. These micrographs where selected in order to show a representative image of the observed structures – the magnification may differ in order to highlight certain areas of interest. As can be seen in Figure 14, structurally the feed material (B) does not differ much from the hydrochars itself, but on the surface of the particles already at a magnification of 200x carbon spheres are visible (Figure 14, red arrows).

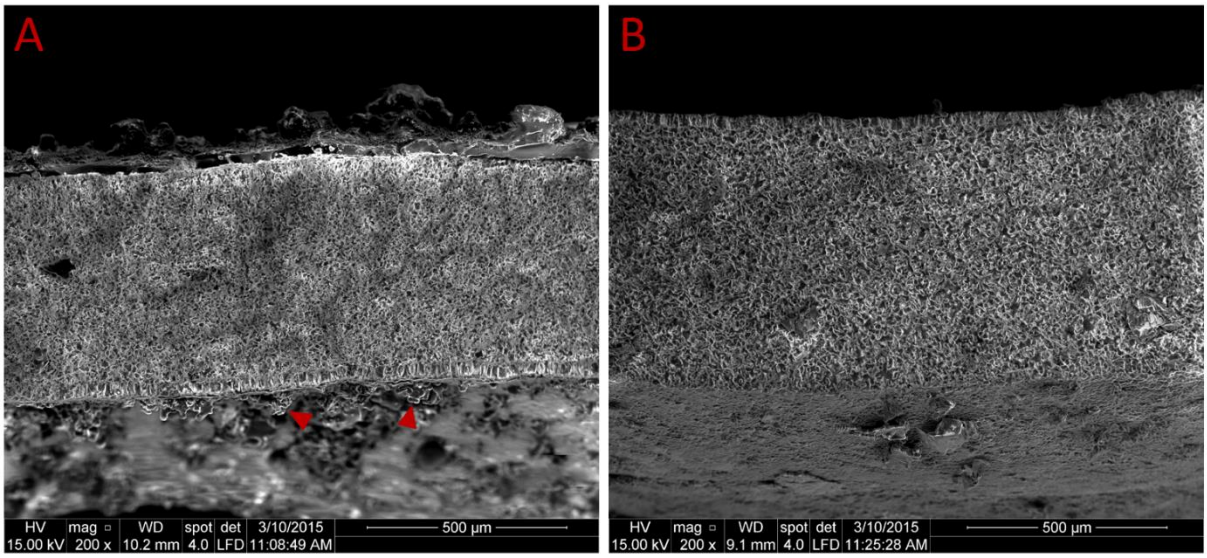

Figure 14. SEM micrographs: cross section of pistachio shells (A) carbonised at 180°C for 12h and (B) untreated. The red arrows indicate the carbon spheres found on the surface of hydrochars.

Also bamboo sticks do not show great structural changes due to hydrothermal treatment (see Figure 15 A and B). Basic components of bamboo, including parenchyma cells (red arrows), fibre bundles (blue arrows) and vessels (yellow arrows) are still present after hydrothermal carbonisation.

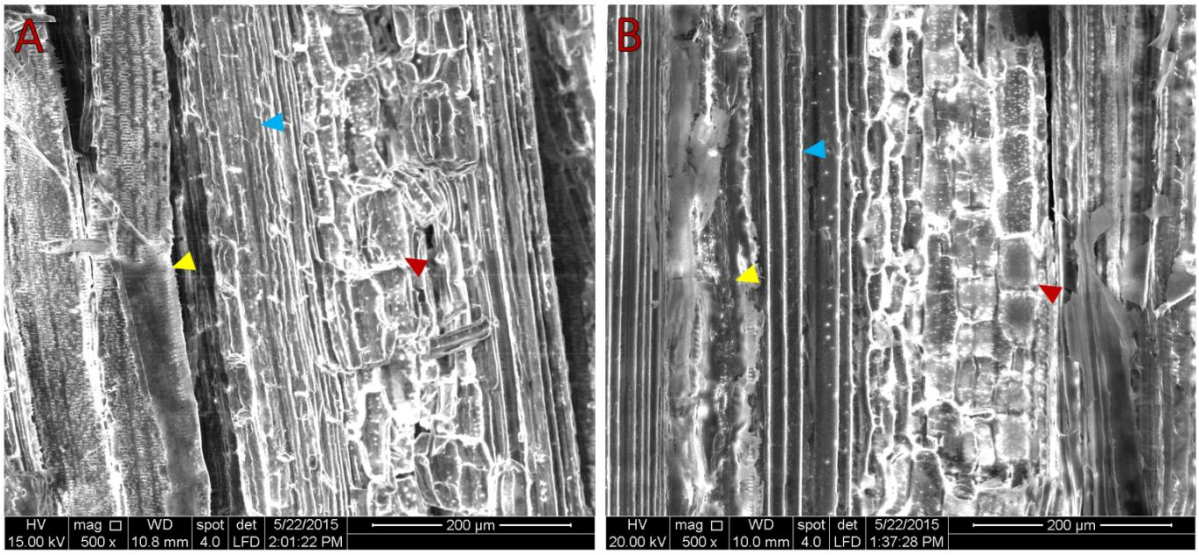

Figure 15. SEM micrographs: longitudinal cross section of bamboo sticks (A) carbonised at 180°C for 2h and (B) untreated. Arrows are indicating the following structural components: parenchyma cells (red), fibre bundles (blue) and vessels (yellow).

On higher magnifications (1000x, 3500x) abundant spherical particles were detected on carbonised pistachio shells obtained at different residence times (Figure 16 A and B). These spheres have a mean diameter of 7.10 ± 1.64 µm and show a low variance in size.

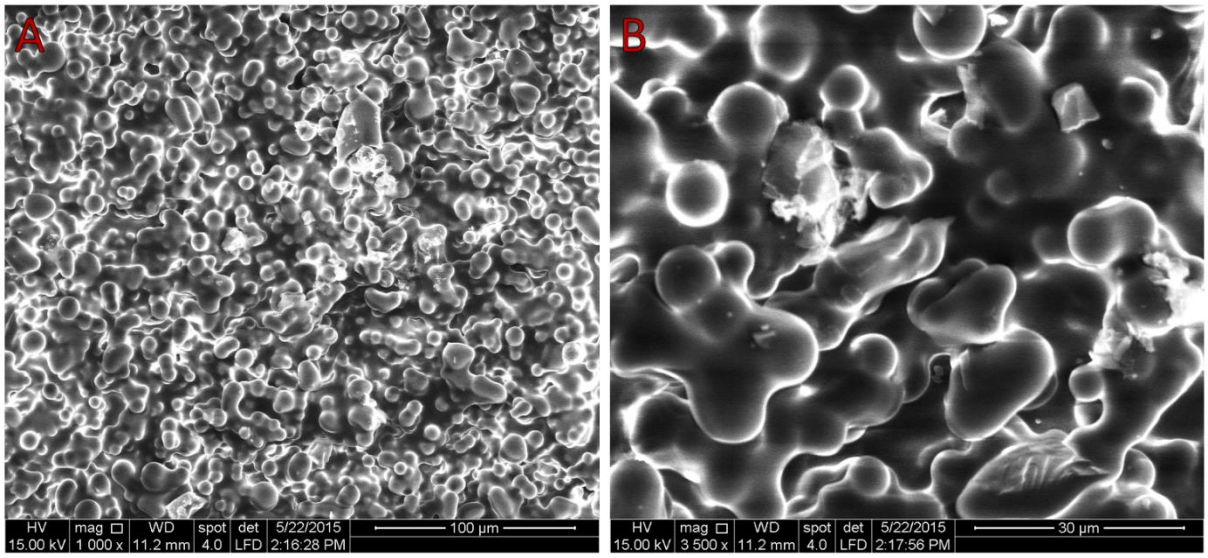

Figure 16. SEM micrographs: spherical carbon particles on the surface of carbonised pistachio shells (180°C, 12hours) – (A) 1000x, (B) 3500x.

Spherical particles on carbonised bamboo sticks instead showed great variances in size and shapes with diameters ranging from 1.82 ± 0.89 µm to 24.12 ± 1.97 µm (see Figure 17).

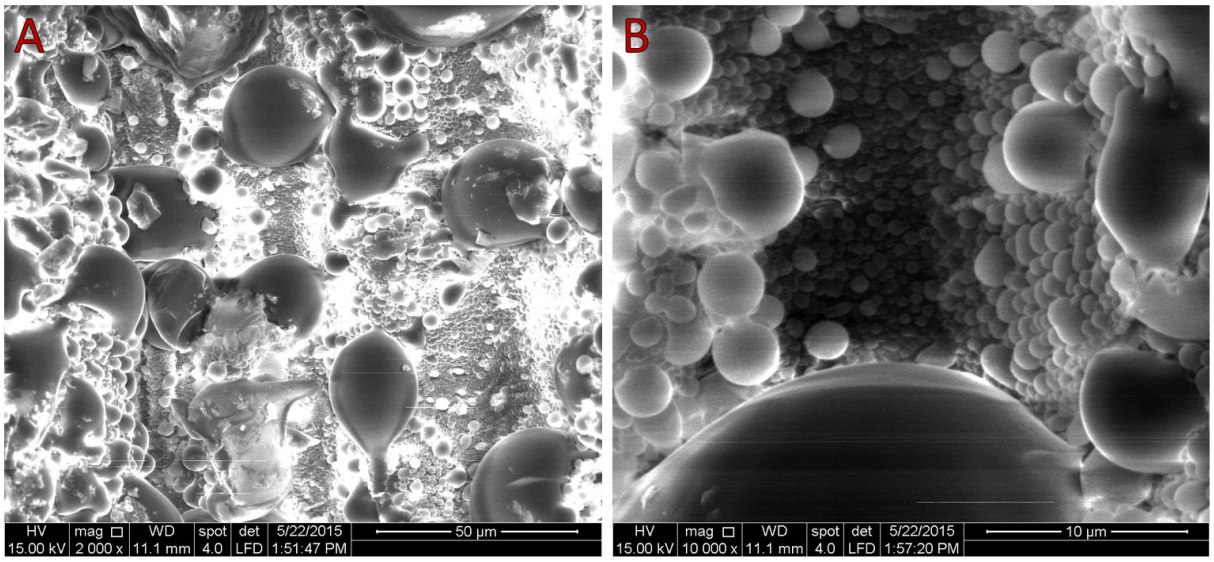

Figure 17. SEM micrographs: spherical carbon particles on the surface of carbonised bamboo sticks (180°C, 2 hours) – (A) 2000x, (B) 10000x.

As expected, also fir needles show similar behaviour under hydrothermal conditions: structurally the needle is still intact and the surface is covered with micro sized carbon spheres (see Figure 18 A and B).

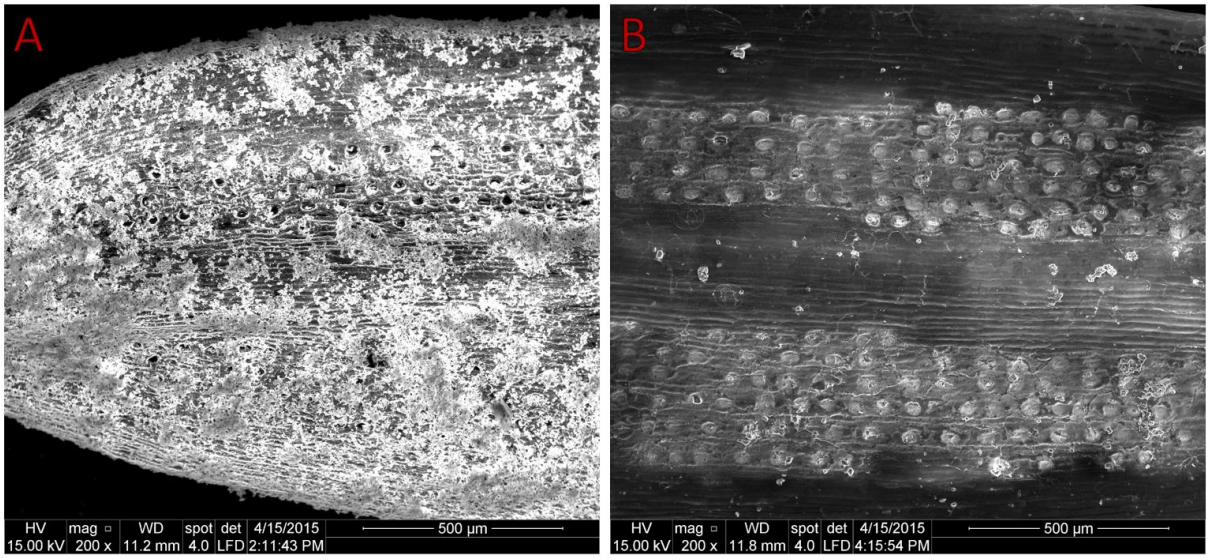

Figure 18. SEM micrographs: fir needle (A) carbonised at 180°C for 1h and (B) untreated.

The mean diameter of the carbon spheres obtained from Figure 19 was estimated to be 2.97 ± 0.70 µm.

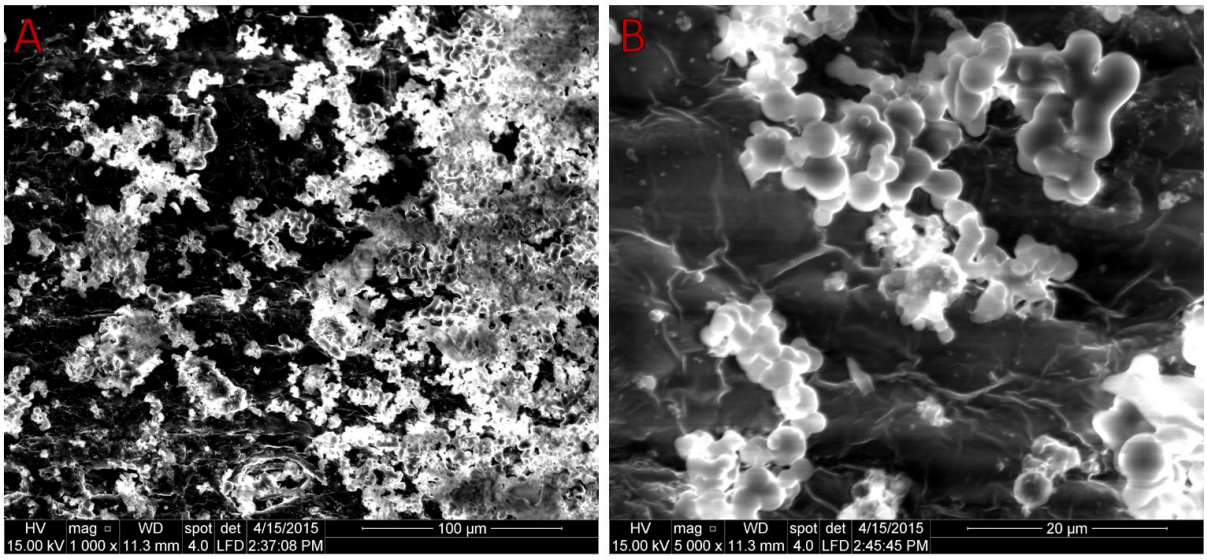

Figure 19. SEM micrographs: spherical carbon particles on the surface of carbonised fir needles (180°C, 1 hour) – (A) 1000x, (B) 5000x.

Dried biogas slurry and its HTC product resulted in low image quality, most probably because the material offered a low conductivity and chemical analysis suggested a high inorganic content (data not shown).

3.2 Molar O/C Gradient of Cross Sections

This chapter is focusing on pistachio shells and bamboo sticks, since those feed materials had the best structural properties for EDX analysis. By measuring molar O/C profiles on cross sections of pistachio shells (native, 1 hour, 6 hours and 12 hours) the following data could be obtained (see Figure 20). The untreated pistachio shell shows a flat concentration profile at an average value of 0.764±0.006 atomic percent (a%), which is in the range of the chemical analysis (0.74 a%) performed in previous studies (Madner 2014). Carbonised pistachio shells instead show a decline in O/C concentration from the centre of the particle to its surface. It can be seen that the residence time influences the overall carbonisation of the particle by lowering O/C concentration profiles.

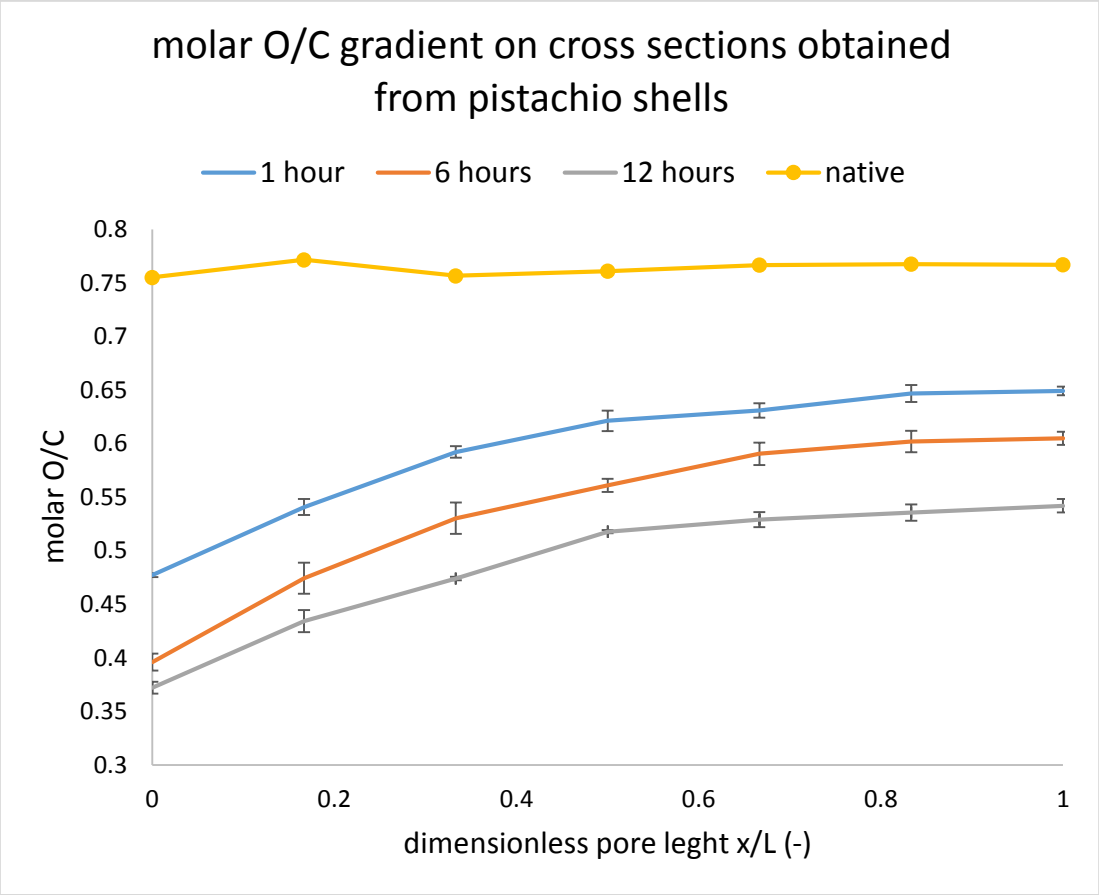

Figure 20. Molar O/C profiles obtained from pistachio shells. Error bars indicate the mean standard deviation (n=3).

Furthermore, it is shown that the greatest change in concentration is achieved in the first hour of carbonisation. The lowest concentration 0.372±0.005 a%, was found on the surface of particles treated for 12 hours, where at the same time the core only achieved 0.542±0.006 a%. Compared to the chemical analysis of the same batch: 0.52 a% (Madner 2014), it shows that the mean concentration of the material is slightly lower than the core concentration measured with EDX.

In addition, the same method was used to measure O/C profiles of native and carbonised (2 hours) bamboo sticks. The resulting profiles show a decline in O/C concentration from the centre of the particle to its surface (see Figure 21), which correspond to the results from pistachio shells. Unfortunately only one residence time was analysed, due to modifications of the reactor.

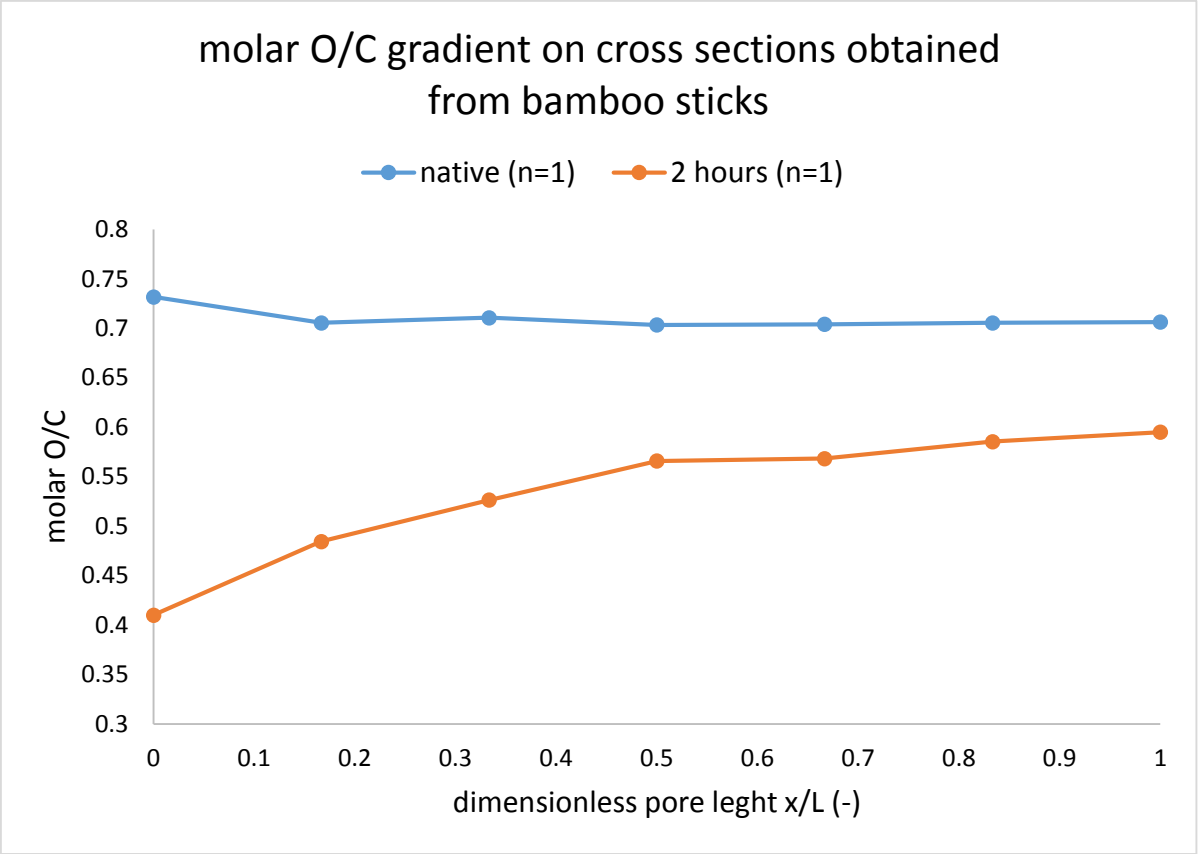

Figure 21. Molar O/C profiles obtained from bamboo sticks.

Figure 21 also shows, that the average O/C concentration of native bamboo sticks 0.710±0.010 a%, which is lower compared to pistachio shells. Regarding particle sizes of pistachio shells (0.63 mm thickness) and bamboo sticks (4.1 mm in diameter) it seems that the 6.5x increased thickness of bamboo sticks did not change the characteristic reduction of O/C profiles under hydrothermal conditions.

3.3 C Thiele Module and Effectiveness Factor

In order to further analyse the concentration profiles obtained from pistachio shells, the data was fitted to the Thiele module as explained in chapter 2.3.4 and thereby the Thiele modules could be calculated by least square regression (Figure 22).

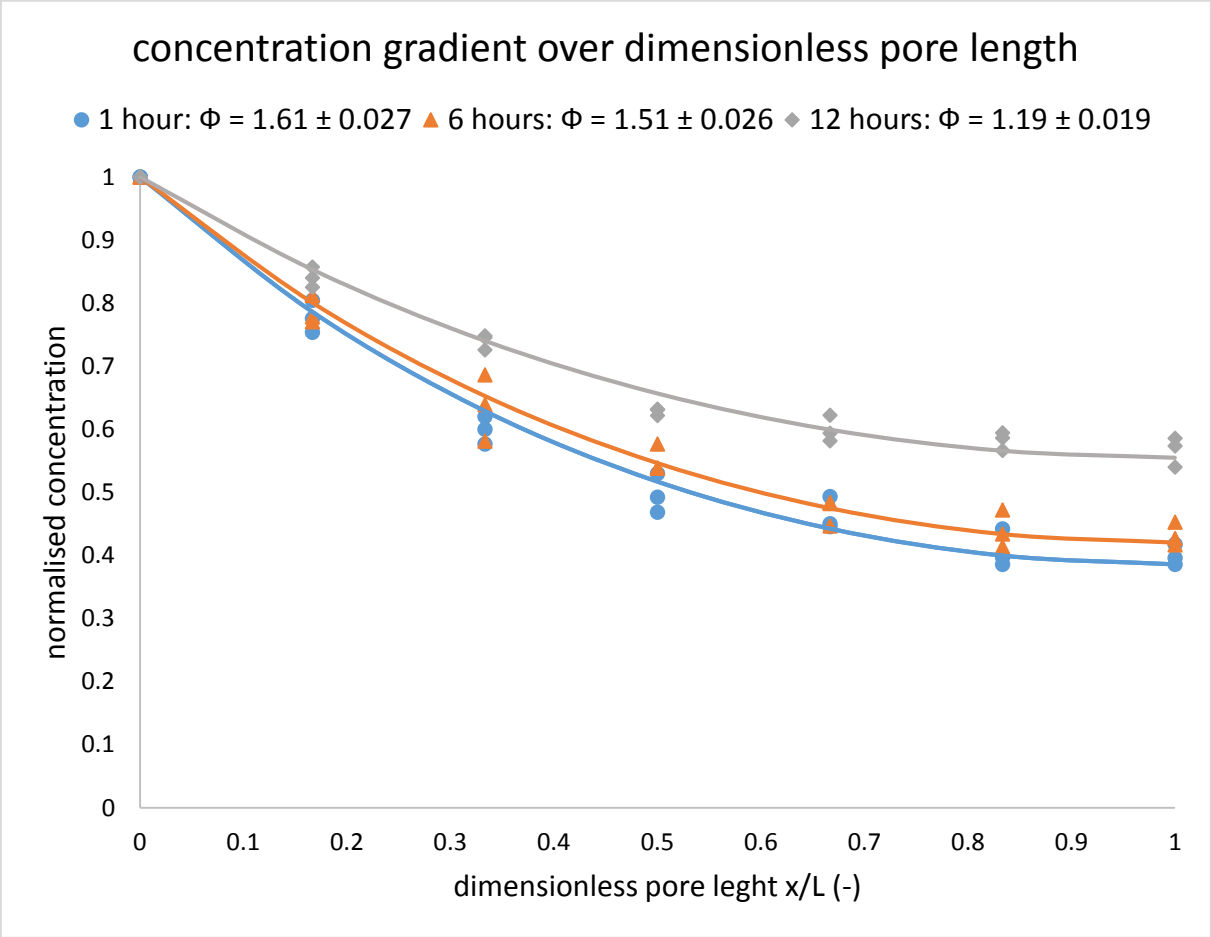

Figure 22. Normalised concentrations from pistachio shells over dimensionless pore length at different residence times. Calculation of Thiele module regarding Equation 6.

In Figure 22 it can be seen that in a timeframe of 1 to 12 hours, the Thiele module Φ is reduced from 1.61 ± 0.027 to 1.19 ± 0.019. In addition, a greater change of Φ was observed after 6 hours. By converting the Thiele module into the effectiveness factor η, this behaviour is more apparent (Figure 23).

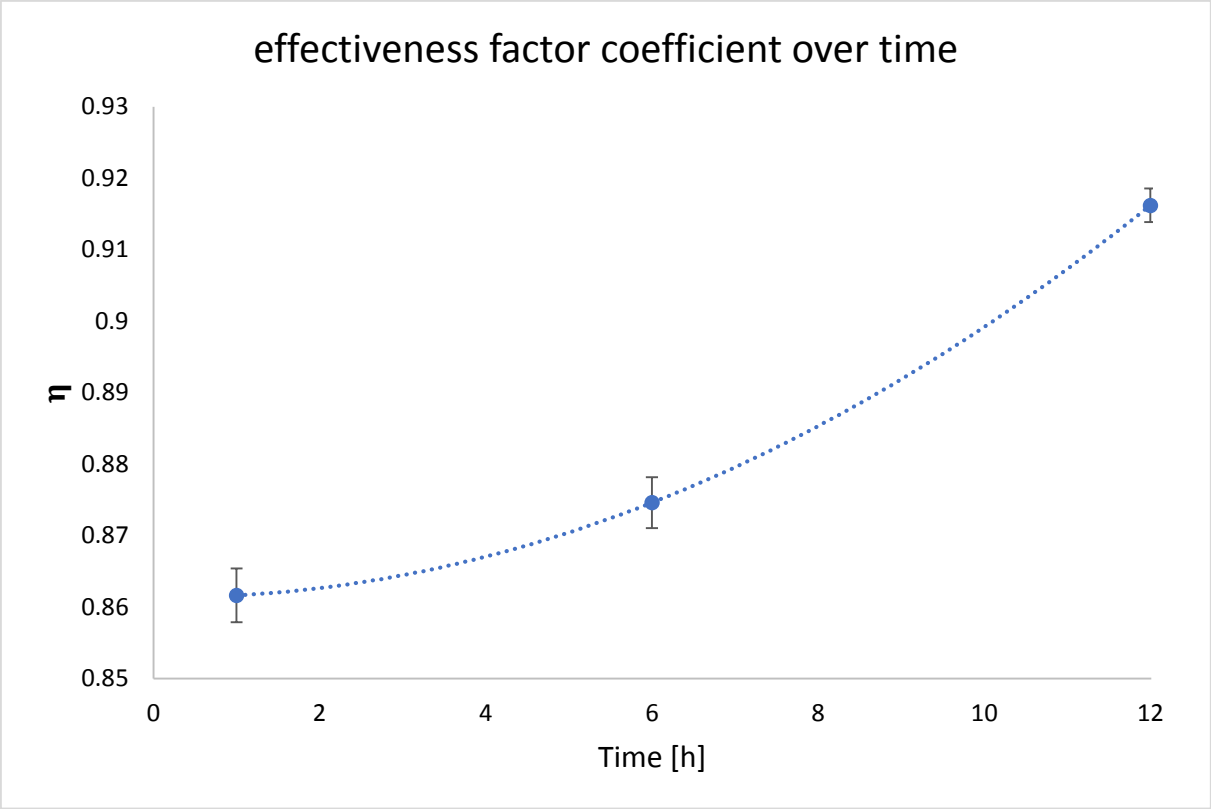

Figure 23. Effectiveness factor η over time converted from the Thiele modules of 3 different residence times obtained from pistachio shells. Error bar indicate the mean standard deviation (n=3), the dotted line represents a 2nd polynomial trend line.

The effectiveness factor η, which is known as the factor which decreases the intrinsic reaction rate by diffusion is plotted over time. It can be observed, that the effectiveness factor changes from 1 to 12 hours as 0.8616±0.0038, 0.875±0.0035 and 0.914±0.0024 respectively. In other words, this suggests, that pistachio shells with a mean thickness of 0.63 mm and the same chemical composition reduce the intrinsic carbonisation reaction by nearly 14% in the first hour. Whereas bamboo sticks show an effectiveness factor of 0.874±0.0035 at 2 hours (see Figure 24) but with a much larger particle size (4.1 mm in diameter).

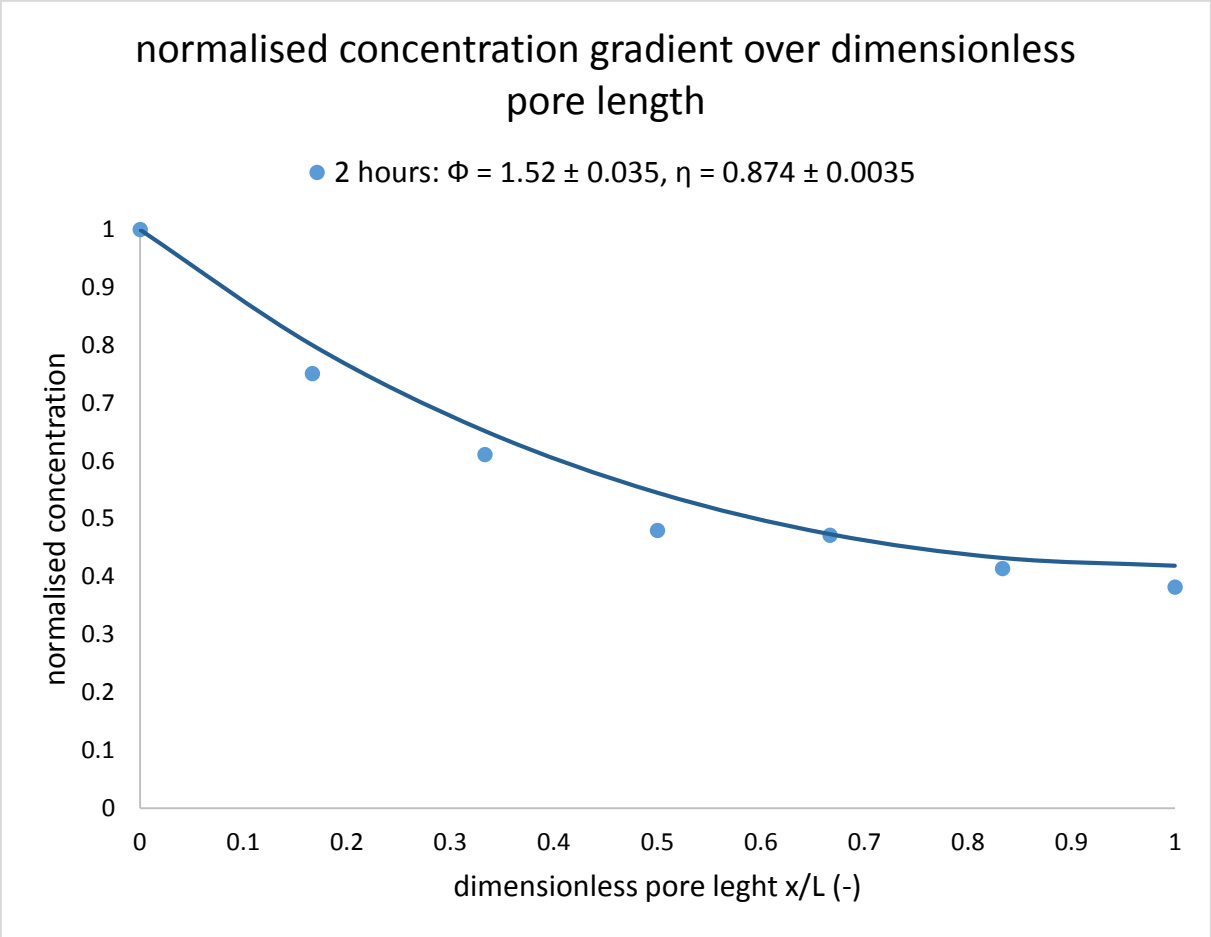

Figure 24. Normalised concentrations from bamboo sticks over dimensionless pore length at a residence time of 2 hours. Calculation of Thiele module regarding Equation 6.

4. Discussion

Since it was the first time that a structural analysis with SEM was performed with hydrochars obtained from this HTC reactor, the observation of carbonaceous spheres was important. Their presence is unique for the HTC process (see chapter 1.4.4) and therefore they can serve as an additional proof that hydrothermal reactions occur with the selected process parameters. Furthermore, chemical analysis with EDX is a frequently used method to determine O/C ratios of hydrochars, but the analysis of O/C profiles in combination with the Thiele module is most probably a new approach to determine the influence of diffusion. This approach was primarily influenced by an experiment performed by Reza et al. 2013 where Thiele modules of Loblolly pine particles (0.88-2.1 mm in diameter) where determined by analysing the mass yield of the threated biomass. Since his experiment was performed at

230°C and rather short residence times, the results cannot directly be compared. But the resulting Thiele modules: 1.7 (8.8 mm in diameter) – 2.4 (2.1 mm in diameter) do correlate with the results of this study – the higher Thiele modules can be explained by a different feed material, higher reaction temperature and lower residence times.

Another important finding of the structural analysis, was that the observed structural changes of the feed materials during the hydrothermal process were less than macroscopic appearance would suggest. This contributes to the fact that lignocellulosic biomass does not fully degrade under hydrothermal condition and especially selected parameters of 180°C. This was also an important assumption for building the model, since the Thiele module is based on heterogeneous catalysis, the non-degradable part of cellulose and lignin is assumed to be the inert solid matrix.

The chemical analysis with the Energy Dispersive X-ray detector showed first of all an acceptable correlation with the chemical analysis of the same materials performed by D. Madner (2014). Secondly the molar O/C profiles give an insight into the carbonisation reactions which are happening on the inner surface of the biomass particles. Thereby it can be assumed, that biomass particles in general are carbonised from the surface to the centre of the particle.

Furthermore, the O/C concentration is continuously lowered over a time span of 12 hours, but the greatest reduction happened in the first hour. This contributes to the idea that hemicellulose and extractives are degraded or extracted within minutes (see chapter 1.4), and thereby drastically reducing O/C molar ratios of the material. It could also be shown, that the influence of diffusion is reduced over time, which indicates, that either the reaction constant is lowered, and/or the diffusion coefficient is increased. Most probably both factors change over time, but it is more obvious that ongoing hydrolytic reactions are increasing the porosity of the cellulosic material and therefore increasing the diffusion coefficient. Unfortunately this reduction is less than expected, and at the moment, long residence times do not seem to be applicable for processes in industrial scale. Also D. Madner (2014) came to the conclusion, that the increased heating value of hydrochars obtained at longer residence times (>1 hour) do not justify the higher heating and equipment costs for keeping the temperature constant. Nevertheless the influence of diffusion has to be considered for further development - especially for feed materials with higher particle sizes e.g. woody materials, agricultural

wastes or municipal wastes. Regarding the process design, a continuously stirred tank reactor may have the potential to increase the efficiency of the process by agitating the subcritical fluid.

The above mentioned assumptions, are drawing the attention to the first hour of the hydrothermal process, where O/C ratios are rapidly decreasing and heating values of the dried hydrochar rapidly increase (Madner 2014; Reza et al. 2013). The use of shorter residence times could make a continuous process realisable, where feed material is continuously fed into a tubular reactor against the saturation pressure of water at selected temperature – thereby exploiting the exothermal carbonisation reaction (see chapter 1.4) and thereby reducing heating and equipment costs.

Finally, a comparison of two different feed materials (bamboo sticks with pistachio shells) was performed. Unfortunately only one batch with bamboo sticks was performed, since the reactor itself was modified and thereby resulting hydrochar would not be comparable. Nevertheless, it could be shown, that O/C profiles undergo a similar reduction during the hydrothermal process. Furthermore, the experiment shows, that the increased particle size of bamboo, did not affect the Thiele module. This contradicts the model, since with increasing particle size, the effectiveness factor should decrease, but in this case the higher hemicellulose content of the feed material (see chapter 2.2, bamboo sticks) and its structure most probably has a higher influence on diffusivity and reactivity than the particle size. This finding confirms the general assumption that feed material and temperature are the most important factors in HTC.

5. Summary & Outlook

The outcome of this study can be summarised as follows:

- It could be shown, that structural changes of biomass under hydrothermal conditions are visible with SEM analysis, but were less than macroscopic appearance would suggest.
- Chemical analysis shows, that the hydrothermal carbonisation of lignocellulosic biomass such as pistachio shells and bamboo sticks is influenced by diffusion since analysed Thiele modules range from 1.61 ± 0.027 to 1.19 ± 0.019.
- As a consequence, reaction rate are reduced and the process of hydrothermal carbonisation is less efficient – this influence eventually can be reduced by stirring the fluid inside the reactor during the process.
- In addition, even though reactions are occurring over the whole time span of 12 hours, results do highlight the first hour of the hydrothermal process, where the most drastic change in atomic O/C ratio was observed.
- After analysing different organic materials (pistachio shells, bamboo sticks, fir needles and biogas slurry) it can be concluded, that the influence of the feed material is crucial for product properties. Therefore more research on HTC of biomass is needed in order to establish an efficient and sustainable process.

For further research in this field, I suggest the following approach:

- The research should be focused on first hour of the process.
- At the same time the investigation of different feed materials should be expanded in order to limit the influence of diffusion to a certain range and to observe the behaviours of reducing molar O/C ratios by HTC.
- For the selection of feed materials, the following materials properties should be avoided, when combined with SEM-EDX:
  - wet materials
  - materials with an high inorganic content
  - low conductive materials

  - materials, with inhomogeneous consistency and an uncharacteristic surface topography
- Further, different particle sizes should be analysed with this method in order to see, if the measured Thiele modules reach expected values.
- In addition, this EDX based method could be compared with a chemical analysis – by analysing layer after layer of a particle, concentration profiles may can be determined and used for the calculation of Thiele modules.
- An advantage of the before mentioned method is the possibility to analyse also H/C profiles – thereby the data would be more complete, since the two axes of the Van Krevelen diagram could be determined.
- At last I suggest to determine, how strong the influence of agitation (stirred tank) on the Thiele modulus is.

Finally, the findings of this thesis do contribute to the development of hydrothermal carbonisation processes and the method elaborated in this study may be used for further analysis of hydrochars and its feed materials.

List of abbreviations:

Acronym	Definition
A_P	area of the particle
D_{eff}	diffusion coefficient
V_P	volume of the particle
X_0	characteristic geometric length
$r_{intrinsic}$	intrinsic reaction rate
$r_{observed}$	observed reaction rate
a%	atomic percent
$C_{(X/L)}$	concentration over dimensionless pore length.
C_{native}	mean concentration of the native feed material
C_S	concentration at the surface
EDX	energy dispersive x-ray (spectroscopy)
HMF	5-hydroxymethyl furfural
HTC	hydrothermal carbonisation
IPCC	intergovernmental panel on climate change
k	reaction constant
SEM	scanning electron microscope
TEM	transmission electron microscope
wt. %	weight percent
Φ	Thiele module
η	effectiveness factor

Images

Literature

Antal, M.J., Mok, W.S. & Richards, G.N., 1990. Mechanism of formation of 5-(hydroxymethyl)-2-furaldehyde from D-fructose an sucrose. *Carbohydrate research*, 199(1), pp.91–109.

Apaydin-Varol, E., Pütün, E. & Pütün, A.E., 2007. Slow pyrolysis of pistachio shell. *Fuel*, 86(12-13), pp.1892–1899.

AVA-CO2, 2015. No Title. Available at: http://www.ava-co2.com/web/pages/en/about-ava-co2.php [Accessed August 4, 2015].

Baccile, N. et al., 2009. Structural characterization of hydrothermal carbon spheres by advanced solid-state MAS 13C NMR investigations. *Journal of Physical Chemistry C*, 113(22), pp.9644–9654.

Becker, R. et al., 2013. Hydrothermally carbonized plant materials: Patterns of volatile organic compounds detected by gas chromatography. *Bioresource Technology*, 130, pp.621–628. Available at: http://dx.doi.org/10.1016/j.biortech.2012.12.102.

Bell, D. a, Towler, B.F. & Fan, M., 2011. *Coal Gasification and Its Applications*, Available at: http://www.sciencedirect.com/science/article/pii/B9780815520498100014.

Berge, N.D. et al., 2011. Hydrothermal carbonization of municipal waste streams. *Environmental Science and Technology*, 45(13), pp.5696–5703.

Bergius, F., 1928. Beiträge zur Theorie der Kohleentstehung. *Die Naturwissenschaften*, 16(1), pp.1–10. Available at: http://link.springer.com/10.1007/BF01504496.

Bobleter, O., 1994. Hydrothermal degradation of polymers derived from plants. *Progress in Polymer Science*, 19(5), pp.797–841.

Bobleter, O. & Binder, H., 1980. Dynamischer hydrothermaler Abbau von Holz. *Holzforschung*, 34(2), pp.48–51.

Bridgwater, A. V & Grassi, G., 1991. *Biomass pyrolysis liquids upgrading and utilisation*,

D. Fengel and G. Wegener, W. de G., 1984. Wood—chemistry, ultrastructure, reactions. *Journal of Polymer Science: Polymer Letters Edition*, 23(11), pp.601–602. Available at: http://dx.doi.org/10.1002/pol.1985.130231112.

Falco, C. et al., 2011. Hydrothermal Carbon from Biomass: Structural Differences between Hydrothermal and Pyrolyzed Carbons via 13C Solid State NMR. *Langmuir*, 27(November 2015), pp.14460–14471.

FAOSTAT, 2012. Top pistachio producers worldwide. Available at: http://www.agrostrat.gr/?q=en/node/282 [Accessed August 1, 2015].

Fuertes, a. B. et al., 2010. Chemical and structural properties of carbonaceous products obtained by pyrolysis and hydrothermal carbonisation of corn stover. *Australian Journal of Soil Research*, 48(6-7), pp.618–626.

Funke, A. & Ziegler, F., 2010. Hydrothermal carbonization of biomass: A summary and discussion of chemical mechanisms for process engineering. *Biofuels, Bioproducts and Biorefining*, 4(2), pp.160–177.

Garrote, G., Dominguez, H. & Parajo, J.C., 1999. Hydrothermal processing of lignocellulosic materials. *Holz als Roh- und Werkstoff*, 57(3), pp.191–202. Available at: http://link.springer.com/10.1007/s001070050039.

Green, M.L. et al., 2012. Materials for sustainable development. *MRS Bulletin*, 37(04), pp.303–309.

Hanai, T., 2003. Separation of polar compounds using carbon columns. *Journal of Chromatography A*, 989, pp.183–196.

Hans Bisswanger, 2008. *Enzyme Kinetics. Principles and Methods.*, Available at: http://onlinelibrary.wiley.com/doi/10.1002/9780470048672.wecb159/full.

He, C., Giannis, A. & Wang, J.Y., 2013. Conversion of sewage sludge to clean solid fuel using hydrothermal carbonization: Hydrochar fuel characteristics and combustion behavior. *Applied Energy*, 111, pp.257–266. Available at: http://dx.doi.org/10.1016/j.apenergy.2013.04.084.

Heilmann, S.M. et al., 2011. Hydrothermal carbonization of distiller's grains. *Biomass and Bioenergy*,

35(7), pp.2526–2533. Available at: http://dx.doi.org/10.1016/j.biombioe.2011.02.022.

Hirschon, S. et al., 1991. Hydrothermal functionalities treatment and the oxygen in Wyodak coal. *Fuel*, 70(3), pp.289–295. Available at: http://www.sciencedirect.com/science/journal/00162361/70/3.

Hoekman, S.K., Broch, A. & Robbins, C., 2011. Hydrothermal Carbonization (HTC) of Lignocellulosic Biomass. *Energy & Fuels*, 25(4), pp.1802–1810. Available at: http://pubs.acs.org/doi/abs/10.1021/ef101745n.

Holder, R., 2008. *A Global Reaction Mechanism for Transient Simulations of Three-Way Catalytic Converters*,

Hu, B. et al., 2008. Functional carbonaceous materials from hydrothermal carbonization of biomass: an effective chemical process. *Dalton transactions (Cambridge, England : 2003)*, (40), pp.5414–5423.

Hwang, I.-H. et al., 2012. Recovery of solid fuel from municipal solid waste by hydrothermal treatment using subcritical water. *Waste Management*, 32(3), pp.410–416. Available at: http://dx.doi.org/10.1016/j.wasman.2011.10.006.

IPCC, 2011. IPCC Special Report on Renewable Energy Sources and Climate Change Mitigation Summary for Policymakers. *Intergovernmental panel on climate change*, (May 2011), pp.5–8.

Joo, S.H. et al., 2009. Preparation of high loading Pt nanoparticles on ordered mesoporous carbon with a controlled Pt size and its effects on oxygen reduction and methanol oxidation reactions. *Electrochimica Acta*, 54, pp.5746–5753.

Kang, S. et al., 2012. Characterization of hydrochars produced by hydrothermal carbonization of lignin, cellulose, d-xylose, and wood meal. *Industrial and Engineering Chemistry Research*, 51(26), pp.9023–9031.

Kiessling, J.W. et al., 2009. Der österreichische Wald. *Bundesministerium für Land- und Forstwirtschaft*.

Knox, J.H., Kaur, B. & Millward, G.R., 1986. Structure and performance of porous graphitic carbon in liquid chromatography. *Journal of Chromatography A*, 352, pp.3–25. Available at: http://www.sciencedirect.com/science/article/pii/S0021967301833689.

Koopmans, R.J., 2006. R&D challenges for the 21st century. *Soft Matter*, 2(7), p.537.

Kuster, B.F.M., 1990. 5-Hydroxymethylfurfural (HMF). A Review Focussing on its Manufacture. *Starch - Stärke*, 42(8), pp.314–321. Available at: http://dx.doi.org/10.1002/star.19900420808\nhttp://www3.interscience.wiley.com/cgi-bin/fulltext?ID=113442186&PLACEBO=IE.pdf&mode=pdf.

Lehmann, J., 2007. A handful of carbon. *Nature*, 447(7141), pp.143–144.

Libra, J. a et al., 2011. Hydrothermal carbonization of biomass residuals: a comparative review of the chemistry, processes and applications of wet and dry pyrolysis. *Biofuels*, 2(1), pp.71–106.

Liu, Z. & Balasubramanian, R., 2012. Hydrothermal Carbonization of Waste Biomass for Energy Generation. *Procedia Environmental Sciences*, 16, pp.159–166. Available at:

http://linkinghub.elsevier.com/retrieve/pii/S1878029612005609.

Lu, L., Namioka, T. & Yoshikawa, K., 2011. Effects of hydrothermal treatment on characteristics and combustion behaviors of municipal solid wastes. *Applied Energy*, 88(11), pp.3659–3664. Available at: http://dx.doi.org/10.1016/j.apenergy.2011.04.022.

Lua, A.C., Yang, T. & Guo, J., 2004. Effects of pyrolysis conditions on the properties of activated carbons prepared from pistachio-nut shells. *Journal of Analytical and Applied Pyrolysis*, 72(2), pp.279–287.

Luijkx, G.C.., 1994. Conversion of Carbohydrates and Related Compounds.

Madner, D., 2014. Bestimmung der Reaktionsenthalpien bei der Hydrothermalen Karbonisierung von nachwachsenden Rohstoffen. *TU Wien*.

McCollom, T.M., Ritter, G. & Simoneit, B.R.T., 1999. Lipid Synthesis Under Hydrothermal Conditions by Fischer- Tropsch-Type Reactions. *Origins of Life and Evolution of the Biosphere*, (2), pp.153–166. Available at: http://adsabs.harvard.edu/abs/1999OLEB...29..153M.

Mok, W.S.L. & Antal, M.J., 1992. Uncatalyzed Solvolysis of Whole Biomass Hemicellulose by Hot Compressed Liquid Water. *Industrial & Engineering Chemistry Research*, 31(4), pp.1157–1161. Available at: <Go to ISI>://A1992HN89800026\nhttp://pubs.acs.org/doi/pdf/10.1021/ie00004a026.

Møller, J., Boldrin, A. & Christensen, T.H., 2009. Anaerobic digestion and digestate use: accounting of greenhouse gases and global warming contribution. *Waste management & research : the journal of the International Solid Wastes and Public Cleansing Association, ISWA*, 27(8), pp.813–824.

Möller, M. et al., 2011. Subcritical water as reaction environment: Fundamentals of hydrothermal biomass transformation. *ChemSusChem*, 4(5), pp.566–579.

Mumme, J. et al., 2011. Hydrothermal carbonization of anaerobically digested maize silage. *Bioresource Technology*, 102(19), pp.9255–9260. Available at: http://dx.doi.org/10.1016/j.biortech.2011.06.099.

Murray, J.B. & Evans, D.G., 1972. The brown-coal/water system: Part 3. Thermal dewatering of brown coal. *Fuel*, 51(4), pp.290–296.

Najafpour, G.D., 2007. *Biochemical Engineering and Biotechnology*, Available at: http://www.sciencedirect.com/science/article/pii/B9780444528452500173.

Newbury, D.E. & Ritchie, N.W.M., 2013. Is scanning electron microscopy/energy dispersive X-ray spectrometry (SEM/EDS) quantitative? *Scanning*, 35(3), pp.141–168.

Othman, R., Dicks, A.L. & Zhu, Z., 2012. Non precious metal catalysts for the PEM fuel cell cathode. *International Journal of Hydrogen Energy*, 37(1), pp.357–372. Available at: http://linkinghub.elsevier.com/retrieve/pii/S0360319911020192.

Parshetti, G.K., Kent Hoekman, S. & Balasubramanian, R., 2013. Chemical, structural and combustion characteristics of carbonaceous products obtained by hydrothermal carbonization of palm empty fruit bunches. *Bioresource Technology*, 135, pp.683–689. Available at: http://dx.doi.org/10.1016/j.biortech.2012.09.042.

Peterson, A. a. et al., 2008. Thermochemical biofuel production in hydrothermal media: A review of sub- and supercritical water technologies. *Energy & Environmental Science*, 1(1), p.32.

Polishchuk, a. Y. & Zaikov, G., 1997. *Multicomponent transport in polymer systems for controlled release*,

Pum, D., 2015. *803302 Methods in Ultrastructure Research*, Available at: https://online.boku.ac.at/BOKUonline/wbLv.wbShowLVDetail?pStpSpNr=272982&pSpracheNr=2&pMUISuche=FALSE.

Rahmstorf, S. et al., 2010. Scientific understanding of climate change and consequences for a global deal. *Global Sustainability - A Nobel Cause*, pp.67–80.

Reza, M.T. et al., 2013. Reaction kinetics of hydrothermal carbonization of loblolly pine. *Bioresource Technology*, 139, pp.161–169. Available at: http://dx.doi.org/10.1016/j.biortech.2013.04.028.

Rousset, P. et al., 2011. Enhancing the combustible properties of bamboo by torrefaction. *Bioresource technology*, 102(17), pp.8225–31. Available at: http://www.ncbi.nlm.nih.gov/pubmed/21703854.

Salgado, J.M. et al., 2012. Purification of ferulic acid solubilized from agroindustrial wastes and further conversion into 4-vinyl guaiacol by Streptomyces setonii using solid state fermentation. *Industrial Crops and Products*, 39(1), pp.52–61. Available at: http://dx.doi.org/10.1016/j.indcrop.2012.02.014.

Schneider, D. et al., 2011. Characterization of biochar from hydrothermal carbonization of bamboo. *International Journal of Energy and Environment*, 2(4), pp.647–652. Available at: www.ijee.ieefoundation.org.

Scurlock, J.M.O., Dayton, D.C. & Hames, B., 2000. Bamboo: An overlooked biomass resource? *Biomass and Bioenergy*, 19(4), pp.229–244.

Speight, J.G. & Ozum, B., 2001. *Petroleum Refining Processes*, CRC Press.

Stemann, J., Erlach, B. & Ziegler, F., 2013. Hydrothermal carbonisation of empty palm oil fruit bunches: Laboratory trials, plant simulation, carbon avoidance, and economic feasibility. *Waste and Biomass Valorization*, 4(3), pp.441–454.

Stevens, K.P., 2004. *Energy Dispersive Spectrometry of Common Rock Forming Minerals*,

Su, D.S. & Centi, G., 2013. A perspective on carbon materials for future energy application. *Journal of Energy Chemistry*, 22(2), pp.151–173. Available at: http://dx.doi.org/10.1016/S2095-4956(13)60022-4.

Sykes, P., 1973. *Introduction to Organic and Biochemistry*,

Terrones, M. et al., 2002. N-doping and coalescence of carbon nanotubes : *Applied Physics A*, 74, pp.355–361.

Thiele, W., 1939. Relation between Catalytic Activity and Size of Particle. *Industrial Engineering Chemistry*, 31(7), pp.916–920.

Titirici, M.M. et al., 2007. A direct synthesis of mesoporous carbons with bicontinuous pore

morphology from crude plant material by hydrothermal carbonization. *Chemistry of Materials*, 19(17), pp.4205–4212.

Titirici, M.-M., 2013. *Sustainable Carbon Materials from Hydrothermal Processes*,

Titirici, M.-M. & Antonietti, M., 2010. Chemistry and materials options of sustainable carbon materials made by hydrothermal carbonization. *Chemical Society reviews*, 39(1), pp.103–116.

Titirici, M.-M., Thomas, A. & Antonietti, M., 2007. Back in the black: hydrothermal carbonization of plant material as an efficient chemical process to treat the CO2 problem? *New Journal of Chemistry*, 31(6), p.787.

Vogtländer, J., Van Der Lugt, P. & Brezet, H., 2010. The sustainability of bamboo products for local and Western European applications. LCAs and land-use. *Journal of Cleaner Production*, 18(13), pp.1260–1269.

Wang, Q. et al., 2001. Monodispersed hard carbon spherules with uniform nanopores. *Carbon*, 39(14), pp.2211–2214.

Wiedner, K. et al., 2013. Chemical evaluation of chars produced by thermochemical conversion (gasification, pyrolysis and hydrothermal carbonization) of agro-industrial biomass on a commercial scale. *Biomass and Bioenergy*, 59, pp.264–278. Available at: http://dx.doi.org/10.1016/j.biombioe.2013.08.026.

Wohlgemuth, S.-A. et al., 2012. A one-pot hydrothermal synthesis of sulfur and nitrogen doped carbon aerogels with enhanced electrocatalytic activity in the oxygen reduction reaction. *Green Chemistry*, 14(5), p.1515. Available at: http://xlink.rsc.org/?DOI=c2gc35309a.

Xiao, L.P. et al., 2012. Hydrothermal carbonization of lignocellulosic biomass. *Bioresource Technology*, 118, pp.619–623. Available at: http://dx.doi.org/10.1016/j.biortech.2012.05.060.

Yao, C. et al., 2007. Hydrothermal dehydration of aqueous fructose solutions in a closed system. *Journal of Physical Chemistry C*, 111(42), pp.15141–15145.

Zhang, B., Huang, H.-J. & Ramaswamy, S., 2008. Reaction Kinetics of the Hydrothermal Treatment of Lignin. *Applied Biochemistry and Biotechnology*, 147(1-3), pp.119–131. Available at: http://link.springer.com/10.1007/s12010-007-8070-6.

Zou, L. et al., 2009. Nanoscale structural and mechanical characterization of the cell wall of bamboo fibers. *Materials Science and Engineering: C*, 29(4), pp.1375–1379. Available at: http://dx.doi.org/10.1016/j.msec.2008.11.007.